

## DIPLOMA THESIS ASSIGNMENT FORM

### I. PERSONAL AND STUDY DATA

Surname: <u>Papadiamanti</u>	Name: <u>Athina</u>	Personal number: _____
Assigning Department: Department of Mechanics or Department of Architecture or Department of Hydraulic Structures (select one, for ITAM use Dept. of Mech.) _____		
Study programme: <u>Civil Engineering</u>	_____	
Study branch/spec.: <u>Advanced Masters in Structural Analysis of Monuments and Historical Constructions</u>		

### II. DIPLOMA THESIS DATA

Diploma Thesis (DT) title: <u>Evaluation of the Broumov parish house failure, its causality, and some ideas of remediation</u>	
Diploma Thesis title in English: <u>Evaluation of the Broumov parish house failure, its causality, and some ideas of remediation</u>	
Instructions for writing the thesis: <p>The main goal of the dissertation will be to assess and evaluate the cause of the failure of the parish house, deanery Broumov. The analysis requires not only technical knowledge but also historical, cultural, and investigative knowledge as well.</p> <p>The work will consist of the following parts:</p> <ol style="list-style-type: none"><li>1. It should start with an overview of the historical development of the area.</li><li>2. Followed by inspection of the Broumov deanery real estate. With a focus on failures and their possible causes and determining the material properties of masonry.</li><li>3. The obtained knowledge will lead to the creation of the FEM models, and selection of the loading cases.</li><li>4. By comparing the results of the FEM model and the current state of the structure, the probable causes of the failure are determined.</li><li>5. Recommendation of the next procedure or method of remediation.</li></ol> <p>List of recommended literature:</p> <p>[1] Chodějovská, E., Semotanová, E., &amp; Šimůnek, R. (2015). HISTORICAL LANDSCAPES IN BOHEMIA Regions of Třeboň, Broumov and Praha.</p> <p>[2] Tourism, C. Czech Tourism. Retrieved from Czech Tourism: <a href="http://www.czechtourism.com/c/group-of-broumov-churches/">http://www.czechtourism.com/c/group-of-broumov-churches/</a></p> <p>[3] Czech Hydrometeorological Institute, "Historická data - meteorologie a klimatologie," 2019. [Online]. Available: <a href="http://portal.chmi.cz/historicka-data/pocasi/zakladni-informace">http://portal.chmi.cz/historicka-data/pocasi/zakladni-informace</a>.</p> <p>[4] Borri, Antonio &amp; Corradi, Marco &amp; Castori, Giulio &amp; De Maria, Alessandro. (2015). A method for the analysis and classification of historic masonry. Bulletin of Earthquake Engineering. 13. 10.1007/s10518-015-9731-4.</p> <p>[5] ATENA. (2023). ATENA Engineering Documentation. Cervenka Consulting Ltd. User's Manual for ATENA, (<a href="https://www.cervenka.cz">https://www.cervenka.cz</a>)</p> <p>[6] J. Válek, R. V. (2005). Characterisation of mechanical properties of. Structural Studies, Repairs and Maintenance of Heritage Architecture IX.</p>	
Name of Diploma Thesis Supervisor: <u>Martin Válek</u>	
DT assignment date: <u>14.3.2023</u>	DT submission date in IS KOS: <u>6.7.2023</u> <i>see the schedule of the current acad. year</i>
_____	_____
DT Supervisor's signature	Head of Department's signature

## DECLARATION

Name: Athina Papadiamanti

Email: atpap7@gmail.com

Title of the MSc Dissertation: Evaluation of the Broumov parish house failure, its causality, and some ideas for remediation

Supervisor(s): Pavel Kuklík, Martin Valek, Petr Kabele

Year: 2023

I hereby declare that all information in this document has been obtained and presented in accordance with academic rules and ethical conduct. I also declare that, as required by these rules and conduct, I have fully cited and referenced all material and results that are not original to this work.

I hereby declare that the MSc Consortium responsible for the Advanced Masters in Structural Analysis of Monuments and Historical Constructions is allowed to store and make available electronically the present MSc Dissertation.

University: CTU, Prague

Date: 03/07/2023

Signature:

\_\_\_\_\_

This page is left blank on purpose.

To my sister.

This page is left blank on purpose.

## ACKNOWLEDGEMENTS

First and foremost, I want to thank Dr. Martin Válek for his invaluable help and supervision throughout the thesis. Without his guidance and support, I would not have been able to overcome many of the challenges I faced. His expertise and dedication were instrumental in the completion of this work.

I am also grateful to Professor Petr Kabele for stepping in and providing assistance when I needed it. His willingness to help and collaborate with Dr. Valek in the supervision of my thesis was greatly appreciated. His advice and opinions significantly contributed to the development of my research topic.

I would like to acknowledge Professor Pavel Kuklík, the original supervisor of the thesis. Despite being unable to directly oversee the project due to unforeseen circumstances his continued involvement even from a distance was greatly appreciated.

A special thank you goes to Mr. Radomír Pukl and the team of Cervenka Consulting for their assistance in modeling and resolving various issues that came up during the analysis of different models.

I extend my gratitude to P. ThLic. Martin Lanži, who generously allowed me access to the Broumov parish house, which served as his residence. He provided me with as much information as possible and granted permission to scan all the rooms of the house in order to create a 3D model of the building. His cooperation and openness were crucial to the success of my research.

I am thankful to Dr. Bláha for his insightful advice regarding the roof, which played a significant role in calculating the loads. His expertise and recommendations were instrumental in achieving accurate results.

I would like to acknowledge the SAHC Consortium for allowing me to participate in the Master's program and for providing financial support through a scholarship. I want to express my deepest gratitude to all the professors at UMinho University who made all of us feel like a part of the big family of HMS. Their teachings and guidance not only helped us in completing our theses but also prepared us for our future careers.

A heartfelt thank you goes to all the people I had the pleasure of meeting with during this year, especially those who have become lifelong friends. The moments and experiences we shared during SAHC will forever hold a special place in my heart. I am grateful for the friendship and support that made SAHC a truly unforgettable experience.

Lastly, I want to give the biggest applause and express my appreciation to my family and friends back in Greece, particularly my parents and sister. Their unconditional love, support, and constant encouragement helped me be here today. Without them, I would not have been able to achieve great things and live such incredible experiences. Thank you for everything.

This page is left blank on purpose.

## ABSTRACT

This thesis focuses on evaluating and investigating the Broumov parish house's condition and the factors contributing to its deterioration. The building, dating back to the Baroque era, houses invaluable 14th-century frescoes that have only recently received attention. The goal of this research is to understand the causes of decay, particularly the observed cracking patterns of the interior, and evaluate the situation.

The thesis begins by providing insights into the building's historical background, geometry, and an assessment of the deterioration patterns. To facilitate the analysis, a 3D model of the parish house was constructed using photogrammetric scanning techniques. Then a 2D model of the wall where the most severe cracks are present was created. The analysis of the model was done using ATENA 2D software.

Given the limited information available regarding material properties and soil characteristics, a range of assumptions and hypotheses were explored to uncover the factors contributing to the observed cracking patterns. Based on the findings, recommendations for further investigations and monitoring strategies are put forth to aid in the ongoing preservation and maintenance of the Broumov parish house.

**Keywords:** Cultural heritage, Baroque, masonry building, crack pattern simulation, photogrammetry, structural analysis, monitoring



This page is left blank on purpose.

## ABSTRAKT

### **Title in Czech: Vyhodnocení poruch broumovské fary, jejich příčinné souvislosti a některé náměty na sanační opatření**

Práce je zaměřena na vyšetření a zhodnocení stavu a faktorů přispívajících ke zhoršování stavu fary v Broumově. Budova datovaná do doby baroka obsahuje nedávno objevené fresky nevyčíslitelné ceny pocházející ze 14. století. Cílem této práce je porozumět příčinám zhoršování stavu, zejména příčinám pozorovaných trhlin v interiéru, a vyhodnocení situace.

Práce začíná nástinem historického pozadí budovy, její geometrie a zhodnocení zákonitostí zhoršování stavu. Pro usnadnění analýzy byl sestaven 3D model farního domu pomocí fotogrammetrických skenovacích technik. Následně byl vytvořen 2D model stěny, kde se vyskytují nejzávažnější trhliny. Analýza modelu byla provedena pomocí softwaru ATENA 2D.

Vzhledem k omezeným dostupným informacím o vlastnostech materiálu a charakteristikách půdy byla zkoumána řada předpokladů a hypotéz s cílem odhalit faktory, které přispívají ke vzniku pozorovaných trhlin. Na základě zjištěných skutečností byla předložena doporučení pro další šetření a monitorovací strategie, které mají pomoci při průběžné ochraně a údržbě broumovské fary.

**Klíčová slova:** kulturní dědictví, baroko, zděné stavby, simulace vzniku trhlin, fotogrammetrie, analýza staveb, sledování

This page is left blank on purpose.

## ΠΕΡΙΛΗΨΗ

### **Αξιολόγηση της κατάστασης της ενοριακής κατοικίας της πόλης του Μπρουμόβ**

Στόχος της παρούσας διπλωματικής είναι η αξιολόγηση και διερεύνηση της κατάστασης της ενοριακής κατοικίας της πόλης του Μπρουμόβ και των παραγόντων που οδηγούν σε διάφορες φθορές. Το κτίριο, που χρονολογείται από την εποχή του Μπαρόκ, φιλοξενεί ανεκτίμητες τοιχογραφίες από τον 14ο αιώνα που μέχρι πρότινος δεν έχαιραν ιδιαίτερης προσοχής. Η έρευνα επικεντρώνεται στην κατανόηση των παραγόντων που δημιουργούν τις διάφορες φθορές στην κατασκευή, με ιδιαίτερη έμφαση στο σύμπλεγμα ρωγμών που παρατηρείται στο εσωτερικό και στην αξιολόγηση της γενικότερης κατάστασης.

Η διπλωματική ξεκινά παρέχοντας πληροφορίες για το ιστορικό υπόβαθρο του κτιρίου, τη γεωμετρία του και μια αξιολόγηση των διάφορων φθορών. Για τους σκοπούς της δημιουργίας ενός στατικού μοντέλου, αποτυπώθηκε με τη χρήση φωτογραμμετρικών μεθόδων ένα τρισδιάστατο μοντέλο του κτιρίου. Έπειτα, δημιουργήθηκε ένα δισδιάστατο μοντέλο του τοίχου όπου παρουσιάζονται οι πιο σοβαρές ρωγμές. Για την ανάλυση του μοντέλου χρησιμοποιήθηκε το πρόγραμμα ATENA 2D.

Λόγω ελλιπών πληροφοριών που αφορούν τις ιδιότητες των υλικών της κατασκευής και τα χαρακτηριστικά του υπεδάφους, πραγματοποιήθηκαν διάφορες υποθέσεις και εξετάστηκαν διάφορα σενάρια με σκοπό να βρεθεί ο λόγος εμφάνισης των ρωγμών. Με βάση τα εξαγόμενα αποτελέσματα, γίνονται προτάσεις για περαιτέρω έρευνα και την παρακολούθηση του κτιρίου με σκοπό να προωθηθεί η διατήρηση και συντήρηση του κτιρίου.

**Λέξεις κλειδιά:** Πολιτιστική Κληρονομιά, Μπαρόκ, Κτίριο τοιχοποιίας, Προσομοίωση συμπλέγματος ρωγμών, Φωτογραμμετρία, Στατική ανάλυση

This page is left blank on purpose.

## TABLE OF CONTENTS

1.	INTRODUCTION .....	17
2.	HISTORICAL BACKGROUND .....	19
2.1	Bohemia .....	19
2.2	Broumov .....	21
2.2.1	Geological Condition .....	22
2.2.2	Climatic Condition.....	23
3.	THE PARISH HOUSE .....	25
3.1	Historical Background .....	25
3.2	The Frescos.....	27
3.3	The Geometry of the Building.....	30
4.	DECAY OVERVIEW.....	33
4.1	The Exterior of the House .....	33
4.1.1	Cracks and Deformation.....	34
4.1.2	Detachment .....	34
4.1.3	Material Loss .....	35
4.1.4	Discoloration and Deposit .....	35
4.1.5	Biological Colonization .....	35
4.2	The Interior of the House.....	36
4.3	Conclusion of the preliminary investigation .....	39
5.	PHOTOGRAMMETRY OF THE BUILDING .....	41
5.1	The Scanning .....	41
5.2	The Result .....	42
6.	THE MODEL ANALYSIS.....	45
6.1	Geometry.....	45
6.2	Material Properties .....	46
6.2.1	Masonry Quality Index.....	47
6.2.2	Material Properties for Modelling.....	48
6.3	Current Loading Situation.....	51
6.4	Boundary Conditions .....	54
6.5	Preliminary Analysis .....	55
6.6	Analysis of Different Decay Hypothesis .....	57
6.6.1	Ground Settlement .....	59
6.6.2	Other settlement hypotheses .....	61
6.6.3	Freezing-thaw Circle.....	63
6.6.4	Other freeze-thaw circle hypotheses.....	66
6.6.5	Other types of models tested .....	68
6.7	Conclusion of the Model Analysis .....	69
7.	CONSIDERATIONS FOR AN ACCURATE MODEL.....	71
8.	CONCLUSION.....	73
9.	RECOMMENDATIONS .....	75
10.	REFERENCES .....	79
11.	ANNEX .....	81
11.1	Exterior Damage Mapping.....	81
11.2	Interior Damage Mapping .....	85
11.3	Calculation of the roof's self-weight.....	89
11.4	Calculation of the vaults' attached to the wall load .....	90
11.5	Calculation of the snow 's live load .....	92

## LIST OF FIGURES

Figure 1.1 - Broumov around 1700 AD [1].....	17
Figure 2.1 - Czech historical lands and current administrative regions [3].....	19
Figure 2.2 - Map of current European borders and the Bohemian crown border in the 1500s [4].....	19
Figure 2.3 - Location of Broumov in the Czech Republic.....	21
Figure 2.4 - Broumov Monastery [7].....	21
Figure 2.5 - Broumov Walls [8].....	21
Figure 2.6 - Geological map of Broumov [10].....	23
Figure 2.7 - Köppen climate types of the Czech Republic [13].....	23
Figure 2.8 - The Köppen Climate Classification [14].....	23
Figure 3.1 - Location of the building in the city of Broumov [15].....	25
Figure 3.2 - The reconstruction plans of 1913.....	26
Figure 3.3 - Historical Timeline of the Broumov Parish House.....	27
Figure 3.4 - Floor Plan of the Frescos room separated according to the date of construction assumed by the architectural style.....	27
Figure 3.5 - The frescos of the southwest wall.....	28
Figure 3.6 - The ceiling of the frescos room.....	28
Figure 3.7 - "The Last Judgment" a) the frescos as it appears today, b) Illustration of the fresco made by Michal Čepelka [19].....	29
Figure 3.8 - The main façade of the building a) 2001 [21], b) 2019, and c) 2023.....	30
Figure 3.9 - Floor Plan.....	30
Figure 3.10 - Detail of the roof.....	31
Figure 4.1 – The four façades.....	33
Figure 4.2 - a) Fracture crack near a window, b) craquelè effect.....	34
Figure 4.3 - a) Delamination of Southwest facade, b) Blistering of Southeast facade.....	34
Figure 4.4 - Discoloration on the main façade.....	35
Figure 4.5 - Part of the roof a) main facade, b) northwest facade.....	36
Figure 4.6 - Middle wall.....	36
Figure 4.7 - Cracks mapping on part of the middle wall.....	37
Figure 4.8 - Basement a) Detached wall, b) Inclined staircase.....	38
Figure 4.9 - Moisture on the walls of the first floor.....	38
Figure 5.1 - RICOH THETA 360.....	41
Figure 5.2 - The Matterport application.....	42
Figure 5.3 - Overview of the 3D Model.....	42
Figure 5.4 - Navigation in the interior and the additional tags for the decay.....	43
Figure 6.1 - Plan view of the wall and the total thickness of the exterior walls.....	45
Figure 6.2 - Simplified geometry of the wall.....	46
Figure 6.3 - Uncovered wall.....	47
Figure 6.4 - Exponential crack opening law [25].....	49
Figure 6.5 - View of the rear facade and the model of this part of the wall.....	50
Figure 6.6 - The model of the basement.....	50
Figure 6.7 - Plan view of the wall with the trusses.....	51
Figure 6.8 - Plan view of the vaults attached to the wall.....	52
Figure 6.9 - The area of the floor supported by each vault.....	52
Figure 6.10 - Table 6.2 of the EN 1991-1-1:2002.....	53
Figure 6.11 - Snow Load Map of the Czech Republic [31].....	53
Figure 6.12 - The condition of the basement of the building.....	54
Figure 6.13 - The springs and their assigned values.....	55
Figure 6.14 - Results of the preliminary analysis (m).....	56
Figure 6.15 - The model with the ground modeled as a rigid material.....	58
Figure 6.16 - The interface between the wall's base and the ground.....	58
Figure 6.17 - The boundary condition for the first 10 steps of the analysis.....	59
Figure 6.18 - The prescribed displacement at the base of the structure.....	60
Figure 6.19 - Results of the settlement analysis (m).....	60

Figure 6.20 - Comparison between the analysis crack pattern and the expected one .....	61
Figure 6.21 - The settlement of the left wall as prescribed displacement .....	61
Figure 6.22 - Comparison between the analysis crack pattern and the expected one (m).....	62
Figure 6.23 - The settlement as prescribed displacement .....	62
Figure 6.24 - Comparison between the analysis crack pattern and the expected one (m).....	63
Figure 6.25 - The upward displacement of the left exterior wall .....	64
Figure 6.26 - Results of the settlement analysis (m).....	65
Figure 6.27 - Comparison between the analysis crack pattern and the expected one (m).....	66
Figure 6.28 - The settlement of the right part as prescribed displacement.....	66
Figure 6.29 - Comparison between the analysis crack pattern and the expected one (m).....	67
Figure 6.30 - The first model .....	68
Figure 6.31 - Settlement analysis with fixed boundary conditions .....	69
Figure 11.1 - Recommended values of $C_e$ and $C_t$ .....	92
Figure 11.2 - Table 5.2 of the EN1 .....	92

## LIST OF TABLES

Table 6.1 – Masonry Quality Index .....	48
Table 6.2 – Mechanical Properties values .....	48
Table 6.3 – Material Properties for the Numerical Model.....	49
Table 6.4 – Material properties for the Interface .....	59



This page is left blank on purpose.

## 1. INTRODUCTION

The Czech Republic is a small country in the center of Europe with a rich cultural heritage dating back centuries. The land has witnessed the rise and fall of various dynasties, each leaving its mark on the architectural landscape. During the reign of the Premyslid dynasty in the 14th century, the Czech states experienced a period of significant growth and prosperity, marked by the construction of numerous buildings and structures across the country [2].

Unlike the modern construction industry, where designs are based on advanced engineering principles and extensive knowledge of materials and subsoil conditions, builders of the past relied on empirical observations and geometrical rules. The early design approaches in the 17th century marked a significant step towards rational construction practices. However, the limited understanding of construction materials and subsoil characteristics meant that historical buildings were often either under-designed or over-designed. Those that have survived to the present day typically fall into the latter category.

Over the course of centuries, these historical buildings have been subjected to various forms of stress, including soil settlement and material deterioration, leading to a range of challenges and issues. In the Czech Republic, the problem of material deterioration, exacerbated by a lack of maintenance, is particularly prevalent. During the communist regime, when people were living on property that they did not own, maintaining these buildings was deemed unnecessary. Also, during that time every aspect of society that had to do with religion was neglected, especially the maintenance of the buildings dedicated to it.

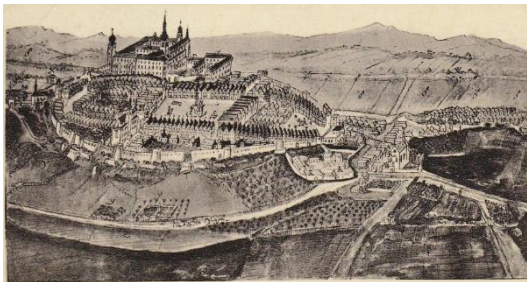


Figure 1.1 - Broumov around 1700 AD [1]

One such building is the Broumov parish house, seemingly a simple structure from the Baroque era. However, hidden within its walls are invaluable 14th-century frescoes that have only recently garnered the attention they deserve. Despite being listed in the State List of Immovable Cultural Monuments of the East Bohemian Region, the building has not received adequate attention or care. Today, it suffers from the

effects of time and decay, with visible cracking patterns appearing on its interior walls.

The goal of this thesis is to investigate the causes of the building's decay, with a particular focus on understanding the underlying factors contributing to the observed cracking patterns. By analyzing the structural and environmental conditions, assessing the quality of materials, and considering historical factors, this study aims to shed light on the deterioration processes affecting the Broumov parish house. Through this research, valuable insights can be gained, enabling the development of appropriate strategies for its preservation and restoration, ensuring the continued appreciation and protection of this cultural treasure for future generations.

This page is left blank on purpose.

## 2. HISTORICAL BACKGROUND

The assessment of a building's condition is closely linked to its historical context and geographical location. This research project focuses on the Parish house located in Broumov, a city in the Bohemian region of the Czech Republic. Over the course of several centuries, both the city and the region have experienced significant historical events, cultural influences, and architectural developments. To gain a comprehensive understanding of the building's current state, it is essential to search its construction history, including the methods employed during its creation, as well as the historical events that took place during its existence. By examining the connections between the building's construction, the evolution of architectural practices, and the historical background of Broumov and the surrounding Bohemian region, this dissertation aims to provide insights into the present condition of the building.

### 2.1 Bohemia

The Czech Republic was originally divided over the centuries into three administrative regions: Bohemia, Moravia, and Czech Silesia (Figure 2.1). Bohemia, the area of interest for this dissertation, occupies the largest part of the Czech Republic. In the past, its borders also included parts of modern-day Germany, Austria, and Poland (Figure 2.2).



Figure 2.1 - Czech historical lands and current administrative regions [3].

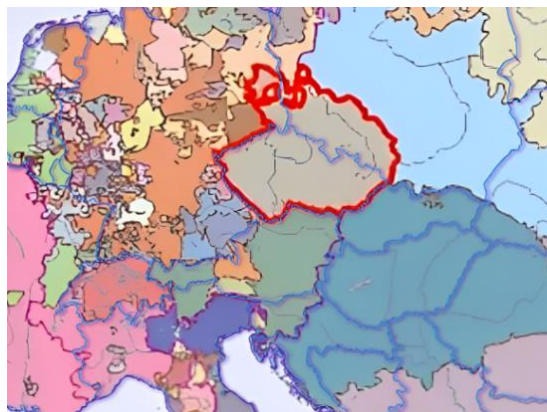


Figure 2.2 - Map of current European borders and the Bohemian crown border in the 1500s [4].

The earliest known inhabitants, who also gave the region its name, were the Celts, known as the Boii. In the late 9<sup>th</sup> century, Bohemia became a part of Greater Moravia, and by the 10<sup>th</sup> century, it was

consolidated under the Přemyslid dynasty [5]. Although Saints Cyril and Methodius introduced Christianity to Bohemia in the 9th century, it took several centuries for it to become the dominant religion.

The first King of Bohemia to also be chosen as Holy Roman Emperor was Charles IV, who ascended to the throne in 1346. Under his reign, Bohemia reached its peak in both political and economic terms. Prague became renowned as the intellectual and cultural center of Central Europe. King Charles IV rebuilt Prague, established Nové Město (New Town), founded Charles University in Prague, and initiated the construction of the bridge spanning the Vltava River.

However, the following centuries were characterized by religious conflicts and political instability. A significant event in Bohemian history was the Hussite Wars, which began in the 15<sup>th</sup> century. The conflict between the Catholic Church and the followers of Jan Hus, a Czech reformer and religious figure, led to a prolonged period of religious and political unrest.

In the 16<sup>th</sup> century, Bohemia became part of the Habsburg Empire and remained under the rule of the Austrian monarchy until the end of World War I. During this period, Czechs struggled to preserve their national identity and culture. The 17<sup>th</sup> century witnessed several dramatic events, including the defenestration of Prague in 1618, which triggered the events leading to the Thirty Years' War between Catholics and Protestants in Central Europe. The war had a significant impact on Bohemia, resulting in the depletion of financial resources, a sharp population decline, and extensive infrastructure destruction [5].

Under Habsburg's rule, Czech nationalism was suppressed, and German became the language of instruction in elementary schools and universities. Efforts to restore the Czech language as the administrative language in place of German began in the late 18<sup>th</sup> century but were unsuccessful.

After World War I, Bohemia served as the foundation for the newly formed nation of Czechoslovakia. The presence of a significant German-speaking population in western Bohemia provided Nazi Germany with a pretext to occupy Czechoslovakia in 1938, and Bohemia became a German protectorate until the Allies restored the Czechoslovak state in 1945. Following World War II, the country came under the political influence of the Soviet Union and the leadership of the Communist Party. Additionally, Bohemia ceased to be an administrative region of Czechoslovakia as the country was no longer divided along historical borders.

In 1993, Czechoslovakia was dissolved, and the Czech Republic and Slovakia became independent states. Bohemia remains one of the regions of the Czech Republic and continues to be an important cultural and economic center in Central Europe.

## 2.2 Broumov

Broumov is a town situated in the northeastern part of the country, close to the border with Poland (Figure 2.3). The town is known for its beautiful Baroque architecture, including the Broumov Monastery (Figure 2.4), founded in the 13<sup>th</sup> century and considered one of the most important historical monuments in the region. Broumov is also surrounded by the scenic Broumov Walls, a series of sandstone formations that are popular among hikers and rock climbers (Figure 2.5) [6].



Figure 2.3 - Location of Broumov in the Czech Republic



Figure 2.4 - Broumov Monastery [7]



Figure 2.5 - Broumov Walls [8]

Broumov has a long and rich history dating back to the Middle Ages. The town was founded in the 13<sup>th</sup> century (1213) by the Benedictine Order, who established the Broumov Monastery as their center of worship and education. The monks played a significant role in the town's development, constructing many important landmarks and contributing to its cultural and economic growth. Notable buildings include the two Benedictine monasteries in Broumov and Teplice nad Metují, a collection of twelve churches and chapels in surrounding villages, the oldest wooden church in Broumov, brick farmhouses, and typical German folk houses [9].

In 1275, Broumov was granted the privilege by King Ottokar II to produce and sell cloth. However, several fires broke out over time, destroying the local castle and the original structures, with the exception of the Church of the Virgin Mary. The castle of Broumov underwent significant reconstruction and expansion by one of the abbots into a monastery complex in 1305 and subsequent years. In 1348, the city was granted privileges by King Charles IV, similar to those of royal towns. The town walls were built between 1357 and 1380.

During the Hussite Wars in the early 15<sup>th</sup> century, Broumov was occupied by the Hussites, a group of Czech religious reformers who opposed the Catholic Church. In the 16<sup>th</sup> century, cloth production

thrived, and until the Thirty Years' War, Broumov was renowned as one of Bohemia's largest producers and exporters. As the city grew wealthier, the use of higher-quality materials, such as stone, became more prevalent in houses construction. The monastery, destroyed in a major fire in 1549, was also reconstructed.

Furthermore, in the aftermath of the Thirty Years' War in the 18<sup>th</sup> century, significant renovations were undertaken in the monasteries, and new constructions, including new stone Baroque churches, replaced the old wooden ones. This development continued into the 19<sup>th</sup> century, when Broumov became an important industrial center, with textile factories and breweries springing up in the area.

However, the prosperity of the 20<sup>th</sup> century was short-lived. After the Munich Agreement in 1938, the Broumov region was divided into Broumov and Teplice. Broumov became part of Hitler's Third Reich, while Teplice was incorporated into the Protectorate Bohemia-Moravia. The division was undone after Germany's defeat in World War II, and the area returned to Czechoslovakia. German inhabitants who did not pledge allegiance to Czechoslovakia were expelled from the country. As a result, the area's population decreased by about two-thirds, rendering many buildings unnecessary as their inhabitants were gone. Additionally, the government's atheist policies in later years led to minimal or no maintenance of the buildings by the locals, particularly the churches. This also explains the current state of disrepair of some buildings.

Today, Broumov is a popular tourist destination, renowned for its rich history, beautiful architecture, and stunning natural surroundings.

### **2.2.1 Geological Condition**

Situated at an elevation of 395 meters above sea level, the city of Broumov finds its geological classification within the Paleozoic era of the Bohemian Massif, as indicated by data provided by the Czech Geological Service. The region is characterized by the presence of various rock types, predominantly encompassing siltstone, and mudstone, occasionally interspersed with fine-grained sandstone deposits. These geological formations contribute to the overall composition and structure of the area, shaping its landscape and geological characteristics.



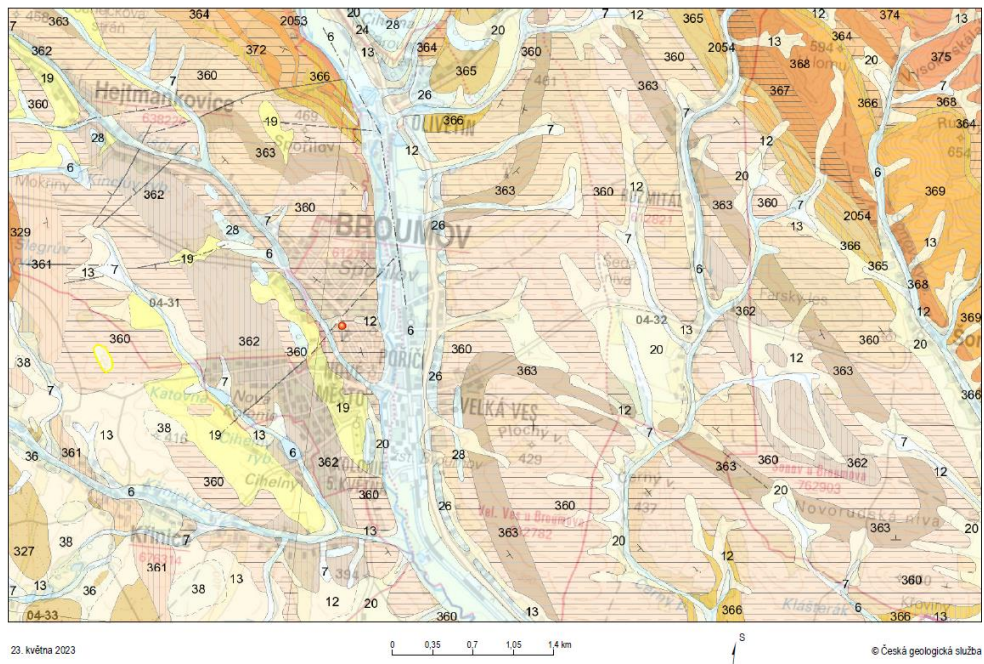


Figure 2.6 - Geological map of Broumov [10]

## 2.2.2 Climatic Condition

The Broumov region is characterized by a cold and temperate climate with notable seasonal variations in temperature, precipitation, and humidity. According to the Köppen and Geiger classification (Figure 2.7), the region falls under the Dfb category (Figure 2.8) [11]. Summers in Broumov are marked by comfortable temperatures, partly cloudy skies, and moderate conditions, while winters bring freezing temperatures, significant snowfall, strong winds, and predominantly cloudy conditions [12].

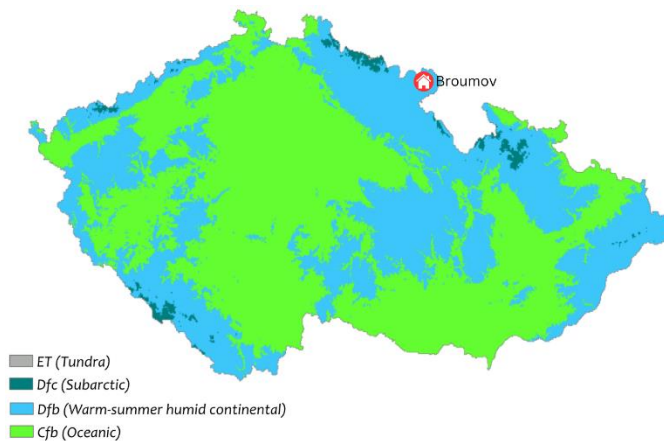


Figure 2.7 - Köppen climate types of the Czech Republic [13]

### Climatic Classifications

Code	Description	Group	Precipitation Type	Level of Heat
Dfd	Extremely cold subarctic climate	Cold (continental)	Without dry season	Very cold winter

Figure 2.8 - The Köppen Climate Classification [14]



The average annual temperature in Broumov is approximately 7 °C, with an average precipitation of 640 mm. Among the months, July stands out as the hottest and wettest, with an average temperature of 16.5 °C and around 10.3 days receiving at least 1.00 millimeters of precipitation. In contrast, January exhibits the coldest temperatures, with an average of -4 °C, representing the lowest mean temperature throughout the year. February emerges as the driest month, with an average of 5.5 days having at least 1.00 millimeters of precipitation. The humidity is muggy, oppressive, or miserable, and does not vary significantly over the course of the year, staying within 1% of 1% throughout. These climatic characteristics contribute significantly to the overall environmental profile of the Broumov region.

### 3. THE PARISH HOUSE

#### 3.1 Historical Background



Figure 3.1 - Location of the building in the city of Broumov [15]

Beside the Church of St. Peter and Paul, attached to the city wall, stands the Parish house. The building did not always serve as the deanery house; this usage began in the second half of the 20th century [16].

The exact date of the building's construction is unknown. However, according to Prof. Jan Royt, the existing frescoes in the building date back to 1330-1340, suggesting that part of the building originates from that time. It is possible that the location once served as a charnel or funeral chapel for the cemetery of St. Peter and Paul Church, which was established alongside the city after 1265.

In 1710, the two-story building we see today was constructed as an extension of the charnel. Its precise function during that period is unclear. In the early 19<sup>th</sup> century, it began to serve as the residence for the bell ringer and church caretaker. By 1851, the cemetery closed following Joseph II's prohibition of burials in inhabited areas and buildings, established in 1784. Experts believe that after the cemetery's abolition, the chamber was filled with human remains and sealed off.

In 1913, there were plans for a complete reconstruction of the Deanery building in the style of the adjacent gymnasium building, this fact suggests that the frescoes were unknown during that period. However, the reconstruction never took place.



Figure 3.2 - The reconstruction plans of 1913

After World War II (1945-1950), under the communist regime's influence to eliminate religious influence, the German Benedictines were expelled from the monastery and settled in Rohr and Lower Bavaria. All services in the monastery ceased until 1950 when the Broumov Monastery became a concentration camp for priests, monks, and nuns from various monastic orders. In 1955, the Parish House that had previously been part of the Monastery was relocated to its current location in the building of the Parish House.

In the summer of 1967, when P. Frantisek Plodek was looking for a place to park his small car, he moved some stored wood in the room and demolished the masonry wall to create more space, leading to the discovery of the paintings. Restoration of the paintings was prepared immediately after the discovery, initially scheduled for 1970 but delayed until 1976. The restoration work continued until 1977 but was left incomplete due to a lack of funds. On April 3, 1979, the building was registered in the State List of Immovable Cultural Monuments of the East Bohemian Region with No. 4420 [17].

In 2012, Professor Jan Royt assessed the paintings and their significance. In 2013-2014, Miroslav Křížek and Pavel Padevět undertook the restoration of the frescoes. The project was financed by the Ministry of Culture and the Hradec Klárové Region.

Finally, in 2019, the building underwent its most recent and significant intervention when the northwest part was demolished and rebuilt with an additional floor. In 2020, the garden in front of the building was reduced in size to facilitate easier access to the fresco hall. During the same year, the room became partially accessible on All-Saint's Day, thanks to donations from the Hradec Klárové Region Council and a married couple of doctors from Broumov. The official opening took place on the Nativity of the Virgin Mary on September 8, 2022, with financial contributions from the European Union, the Hradec Klárové Region, the Hradec Klárové Bishoprpic, and several other donors, both small and large.

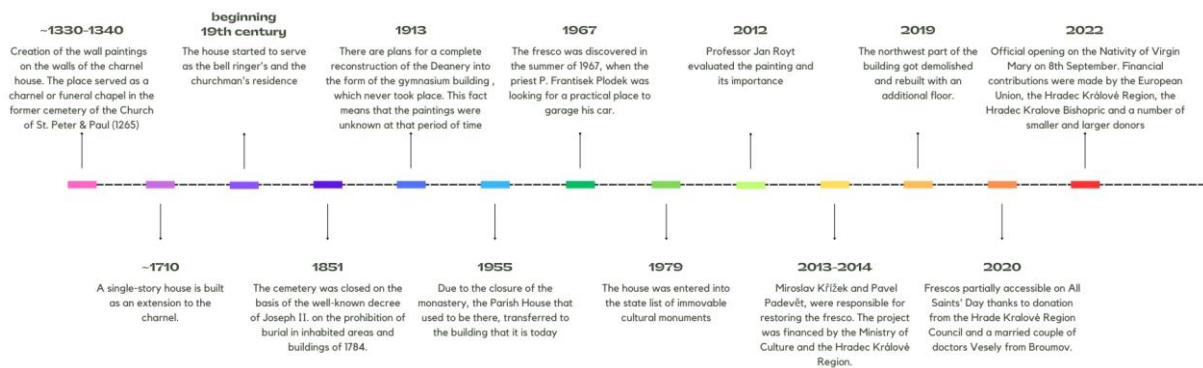


Figure 3.3 - Historical Timeline of the Broumov Parish House

### 3.2 The Frescos

The entire space of the channel can be separated into two parts according to the assumed date of construction as can be seen in Figure 3.4

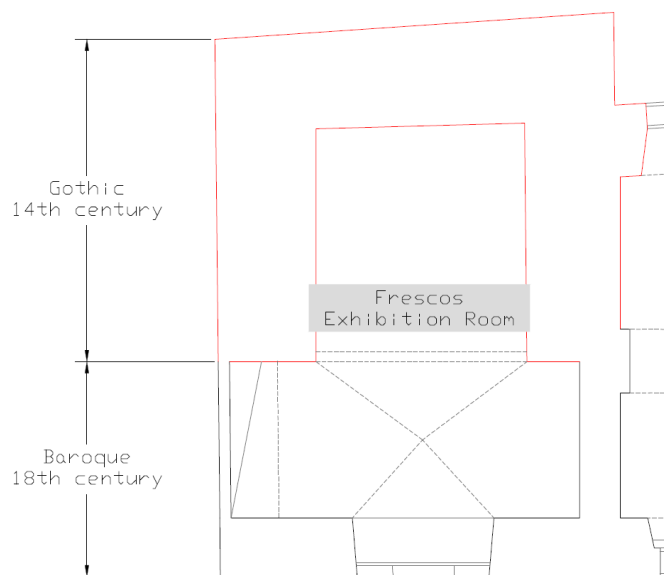


Figure 3.4 - Floor Plan of the Frescos room separated according to the date of construction assumed by the architectural style

The first part with Gothic architectural style consists of a small presbytery, based on an almost square plan, which is covered by a barrel vault. The second one is a larger longitudinal space, with Baroque style arched vault. The floor of the Baroque vaulted chamber is above the level of the floor of the Gothic part, but according to the article “Medieval wall paintings in the basement Broumov Parish House,”<sup>1</sup> even that part of the floor might not be the original floor either, since the paintings begin with just a few centimeters from the ground. A comprehensive archaeological and architectural historical survey is necessary to obtain accurate and thorough information.

<sup>1</sup> Dienstbier, J., Faktor, O., & Royt, J. (2015, February) [18].

All the walls, as well as the ceiling, are covered by fragments of paintings, however, only the one on the southwest side and the ceiling are better preserved.

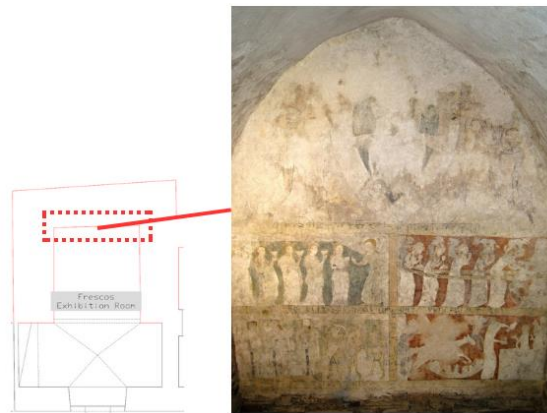


Figure 3.5 - The frescos of the southwest wall



Figure 3.6 - The ceiling of the frescos room

According to the description that was published in the article mentioned before, the medieval wall painting of the presbytery is divided into three bands. As described on the walls of the monument there are 4 main scenes. On the upper band, the primary subject depicted is Jesus Christ in a halo encircling the whole figure. Some figures accompany Him accompanied by St. John the Baptist on the left, the Virgin Mary on the right with an angel behind her holding a cross and a crown of thorns. The 4 Evangelists were presented as symbols and only 2 have survived St. Mark as a lion and St. Luke as a bull. Below that scene is written in capital gothic letters part of Mt 25, 34 "That which is prepared for you from the beginning of the world" [19].

The middle band is a parable about the wise virgins that did good deeds throughout their life, which ensured they with enough oil for their lamps and thus they were prepared for the Last Judgment. The painting is divided into two parts. The left one with the blue background represents heaven and the five wise virgins with their lit lamps are in front of an angel. The right one on the other hand has a red background representing hell. On this side of the painting, five foolish virgins have inverted lamps, a devil is sitting on the shoulder of each one of them and they are surrounded by a large chain getting



dragged into the mouth of Leviathan, the symbol of hell. This kind of illustration is original and has no known analogy.

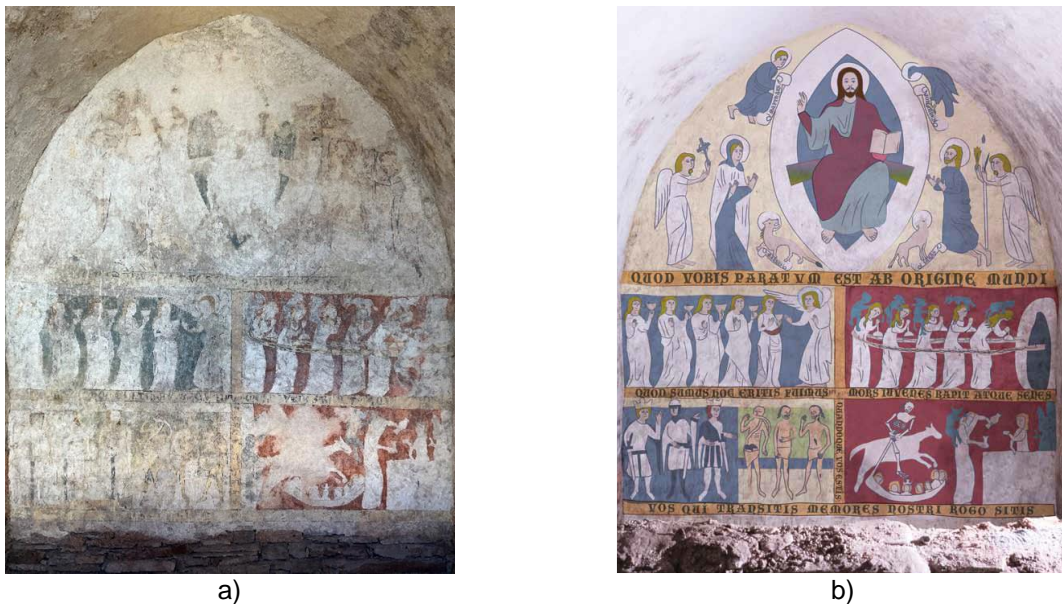


Figure 3.7 - "The Last Judgment" a) the frescos as it appears today, b) Illustration of the fresco made by Michal Čepelka [19]

The last band is also divided into two fields. The scenes are influenced by the then-popular legends. The left on is the meeting of the three living and the three dead, surrounded by the inscription "What we are, so shall you be. What you are, we were too" [20]. On the right part a figure riding a horse, holds the blade of a large scythe, about to cut the heads of the figures of women and men, one of them is wearing a crown. Due to the damage to the painting, it is not possible to determine with certainty who is the figure that is riding the horse, but it is assumed that it is Death personified, because above the painting is written: "Death sweeps away the young and the old". On the far-right corner a woman is pouring herself wine from a jug, which is supposed to represent intemperance and the devil is pulling her from her hair to into the hell. In front of them behind a table stands a sinner.

The last band of the painting is an inscription tape with the writing "I beseech you who pass by, remember us". It is possible that the painting to be continued lower since the original floor should be at least 1.5 m below the current one.

Experts believe that the frescoes are a homogeneous set and that they were made by a single workshop. Although it is obvious that the upper strip was painted by a skilled artist, and the virgins by a not-so-experienced one.

The Broumov frescos belong to the linear style of the first half of the 14th century, their age, style, and iconography have no analogies making their significance go beyond the borders of the region and being classified among the most artistically valuable monuments of wall painting from that period.

### 3.3 The Geometry of the Building

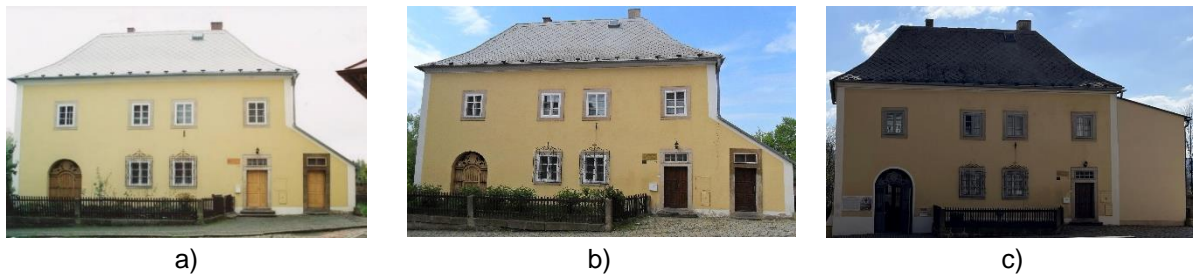


Figure 3.8 - The main façade of the building a) 2001 [21], b) 2019, and c) 2023

The deanery is a two-story building of Baroque architectural style consisting of a basement, ground floor, upper floor, and a gable roof. The layout can be divided into three parts according to the use and the construction dates as presented in Figure 3.9. The overall shape of the building's interior space is nearly rectangular, while the ceilings in all rooms on the first-floor feature vaulted designs.

The left and middle sections of the deanery have retained the original Baroque style from the time of its initial construction. The construction materials employed in these areas include stone masonry for the walls on each floor, brick masonry for the basement vault ceiling, and timber for the construction of staircases. The wall of the southwest part is where the building is attached to the old city wall. The right part which was demolished and rebuilt in 2019 consists of Porotherm 50 bricks and timber beams.

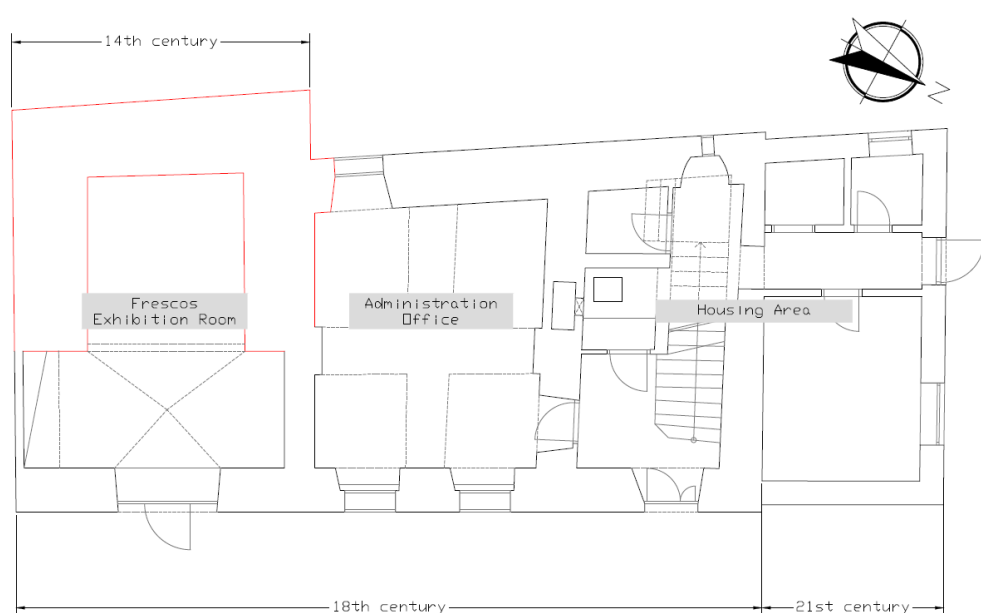


Figure 3.9 - Floor Plan

The inaccessibility of the building's roof made the determination of the geometry of the roof more challenging. To overcome this limitation, expert advice was asked from Dr. Bláha, who specializes in timber roofs of the Baroque era. According to his estimation, the heaviest possible truss would be a baroque truss with a horizontal stool with three full ties. The distance between the trusses for light

covering cannot be less than approximately 1.15 m. The rafters' cross-sections are approximately 13/15 cm and are often laid horizontally. The tie beams, cross braces, vertical and horizontal straps, and longitudinal braces are around 12/14 cm. The main beams should not exceed 18/20 cm. The purlins are about 20/16, usually laid horizontally. Finally, there seem to be quite long rafter sections, which typically have a slightly smaller profile than the rafters, for example, 11/14 cm. The wood used is likely to be spruce. In terms of the roof covering, it seems to be the same as the one of the reconstructed part. As a result, the data provided on the drawings of the newest roof were utilized, which indicated a three-layer structure. The first layer is the roof battens with a thickness of approximately 2 cm and on top of that are placed the tiles. The tiles layer consists of a waterproof asphalt strip with a thickness of approximately 4 mm. The top layer seems to be a diamond shaped geometric pattern of slates.

The use of diamond-shaped geometric patterns of slates on roofs has a long history that dates back centuries. It is difficult to pinpoint an exact starting date for this architectural style, as it has been used in various regions and periods throughout history. Slate is a fine-grained metamorphic rock that can be split into thin, flat sheets. It has been a popular roofing material for centuries due to its durability, low water absorption, and resistance to extreme weather conditions. It can be easily shaped and cut into different sizes and shapes, making it suitable for creating intricate roof patterns. In the context of diamond-shaped patterns on roofs, slates were often cut into rhombus or diamond shapes and arranged in overlapping rows to create the desired design [22].

In Figure 3.10 a detail of the assumed geometry of the roof is presented.

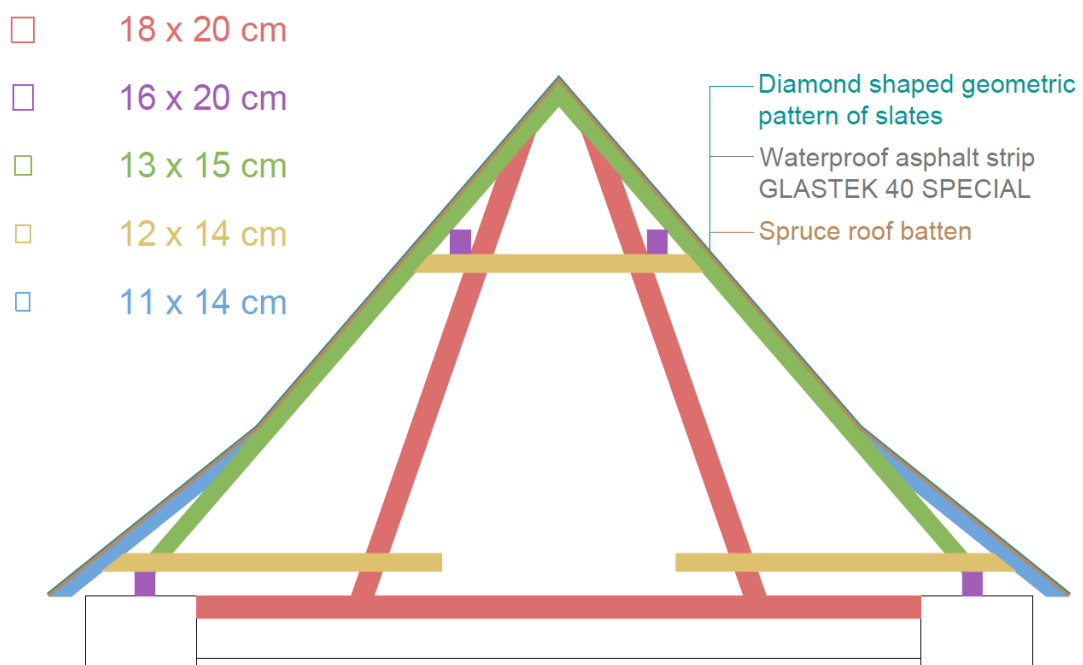


Figure 3.10 - Detail of the roof



This page is left blank on purpose.

## 4. DECAY OVERVIEW

The primary objective of the inspection encompassed the comprehensive mapping of decay, along with the evaluation of the present condition of the building. To achieve this aim, a thorough investigation was conducted, in both the interior and exterior of the structure. In order to classify the observed damages accurately, the guidelines provided by the International Council on Monuments and Sites (ICOMOS) were employed, which identified five main categories: Cracks and Deformation, Detachment, Material Loss, Discoloration and Deposit, and Biological Colonization (ICOMOS-ISCS, 2008) [23].

On the 9th of May 2023, a visual inspection of the building was carried out to assess its condition and identify any visible defects or deterioration. The weather condition was good, with sunshine and an average temperature of approximately 15°C.

### 4.1 The Exterior of the House

Upon the examination that was done, it has been determined that the exterior of the building exhibits no significant damage or deterioration. All the four façades can be seen in Figure 4.1 and their damage mapping is provided in Annex 1. The findings reveal that the majority of the exterior elements remain structurally intact. In contrast, the plaster on the exterior surfaces shows signs of decay. This observation suggests that the deterioration is primarily limited to the superficial layer of plaster rather than affecting the underlying structural elements.



Northeast Façade



Northwest Façade



Southwest Façade



Southeast Façade

Figure 4.1 – The four façades

### 4.1.1 Cracks and Deformation

According to ICOMOS, there are many types of cracks such as fracture, star crack, hair crack, craquelè, and splitting. The façades have some minor fractures on the corners of some windows. The main façade appears to have craquelè cracks on the plaster close to the small garden in front of the building.



Figure 4.2 - a) Fracture crack near a window, b) craquelè effect

### 4.1.2 Detachment

According to ICOMOS guidelines, detachment encompasses various manifestations such as blistering, bursting, delamination, disintegration, fragmentation, peeling, and scaling. In the case of the building's façades, specific issues observed include blistering, delamination, and peeling. Among the façades, the southwest side exhibits the highest level of decay, with large sections of missing plaster. The southeast façade displays widespread blistering issues across its entire surface. On the other hand, the northeast and northwest façades demonstrate no significant detachment problems, apart from minor instances near the area adjacent to the small garden on the main façade.



Figure 4.3 - a) Delamination of Southwest facade, b) Blistering of Southeast facade

### 4.1.3 Material Loss

From all the types of material loss described in ICOMOS alveolization, erosion, mechanical damage, microskarst, missing part, perforation, and pitting none of them appear on the façades of the building

### 4.1.4 Discoloration and Deposit

Discoloration and deposits include coloration, bleaching, moist area, staining, deposits, crust, efflorescence, encrustation, film, glossy aspect, graffiti, patina, soiling, and sub-efflorescence. None of the façades have significant problems with this type of decay. Only the main façade has a small, discolored part of the wall because of the metallic flag case, which is because of the water-licked color on the wall.



Figure 4.4 - Discoloration on the main façade

It is important to note that during the visit, the weather conditions were favorable, with several days prior also experiencing good weather. This circumstance may have concealed certain issues related to humidity or moisture, which may not have been readily apparent upon visual inspection alone.

### 4.1.5 Biological Colonization

Biological colonization, as defined by ICOMOS, is the colonization by plants and microorganisms such as bacteria, cyanobacteria, algae, fungi, and lichen. It also includes influences from other organisms such as animals nesting on and in parts of the building. The roof of the building is the only part where this phenomenon takes place to a large extent, as the whole roof appears to be affected by moss. Something worth mentioning again is that the northwest part was built in 2019, so the organisms grew during the last 4 years.

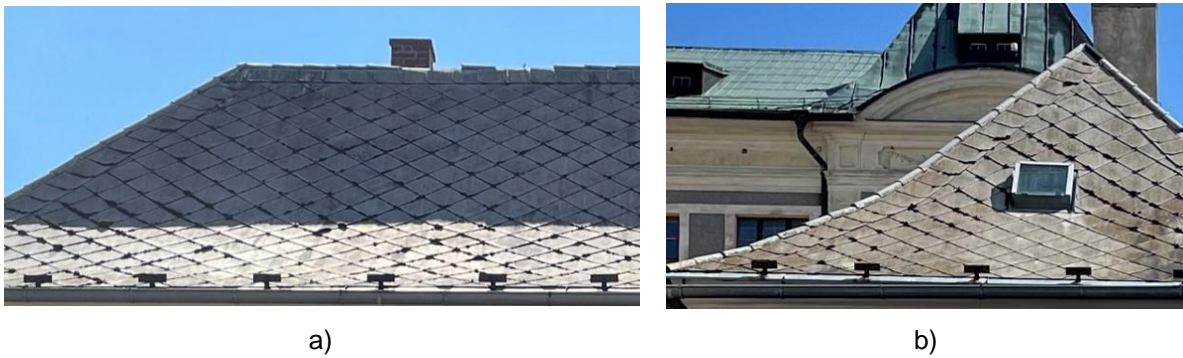


Figure 4.5 - Part of the roof a) main facade, b) northwest facade

## 4.2 The Interior of the House

Within the interior of the building, two primary types of decay are observed. The first type is fractures that as it is depicted in Figure 4.7 are concentrated along the middle wall of the main section of the building (Figure 4.6). A particular concern is the basement, where part of a wall has become detached, and the staircase within the basement area has become inclined. The reason is assumed to be potential ground deformations.

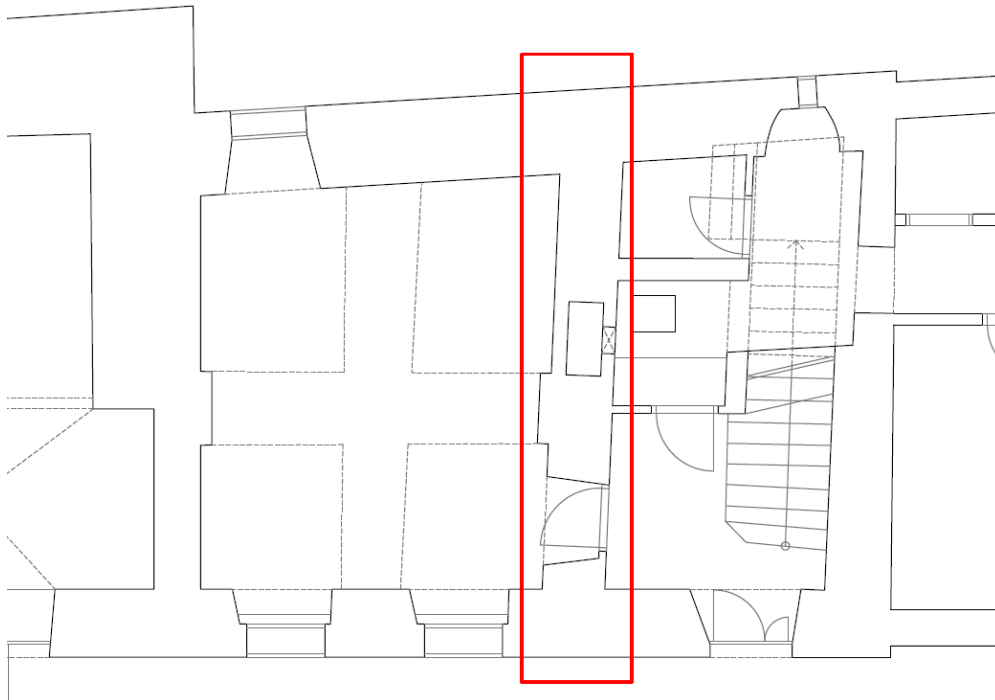


Figure 4.6 - Middle wall



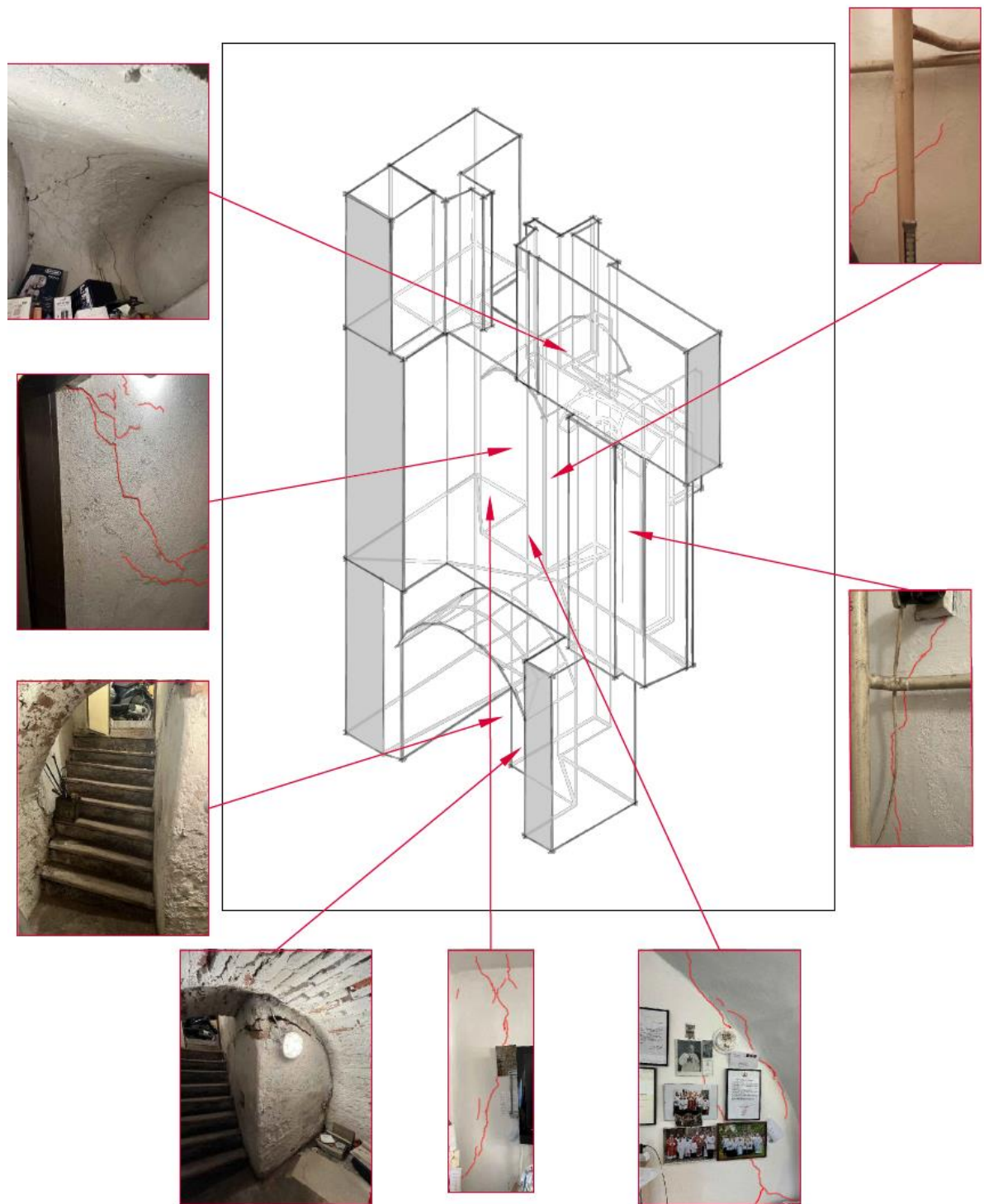


Figure 4.7 - Cracks mapping on part of the middle wall



a)



b)

Figure 4.8 - Basement a) Detached wall, b) Inclined staircase

The second prominent form of decay is the extensive moisture observed primarily on the first floor, particularly in the bedroom and the kitchen areas. The presence of significant moisture infiltration poses a significant concern, as it can contribute to the deterioration of building materials, promoting the growth of mold and mildew. The most possible reason for the existence of moisture is problems on the roof of the building, which was inaccessible for further investigation.

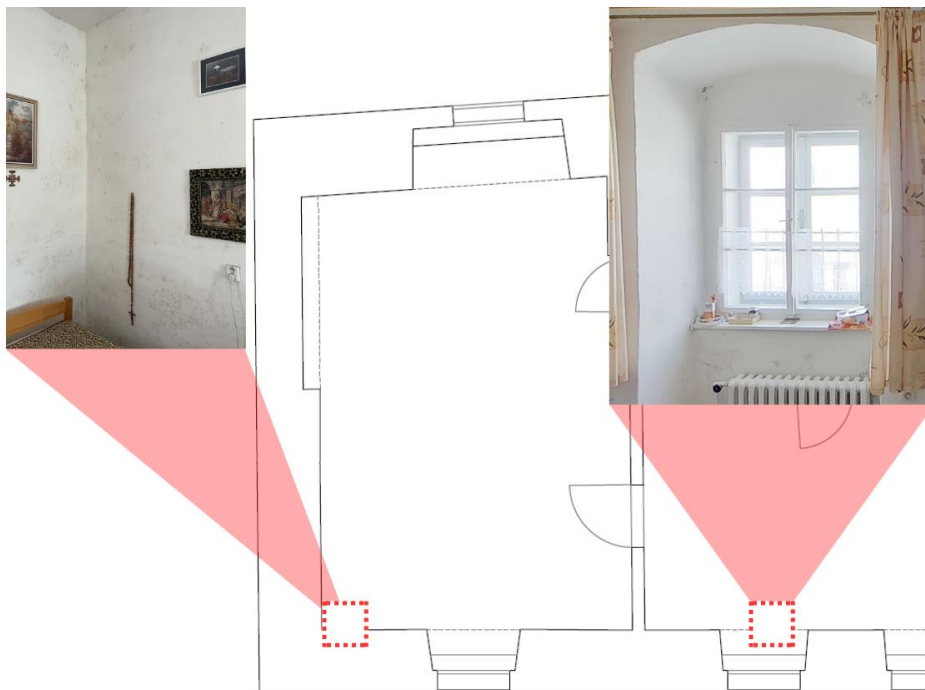


Figure 4.9 - Moisture on the walls of the first floor

The overall decay of the interior is presented in Annex 1.

### **4.3 Conclusion of the preliminary investigation**

Upon assessing the various decay patterns that appear on the building, it has been determined that those present on the exterior are not deemed severe since they appear only on the plaster and the surface of the walls. In contrast, the interior is where the most significant deterioration is observed. The most significant structural damage that affects the building is the formation of a network of cracks along the central wall. According to the information provided by P. ThLic. Martin Lanži during the visit some cracks have also appeared in the church and the school that is located on the same cliff as the Parish House. Based on the factors listed above, it can be assumed that the settlement of the ground is the most probable cause.

Due to a lack of old photographs or previous investigations, there are no clues on the initiation timeline, age, and activity status of the cracks.



This page is left blank on purpose.

## 5. PHOTOGRAMMETRY OF THE BUILDING

As it is mentioned in paragraph 4.3 the building's most significant decay is concentrated on its interior. This observation led to the selection of the middle wall as the focal point for constructing the static model and conducting further investigation. By focusing on this specific element, it was possible to investigate the crack patterns and better understand their causes and implications.

However, the drawings of the building that were initially provided turned out to be lacking important details about the geometry of the interior. This fact led to the decision to proceed with the photogrammetry of the building. By creating a 3D model of the house, it was easier to capture precise measurements, intricate structural elements, and intricate architectural features, ensuring a comprehensive understanding of the building's design.

### 5.1 The Scanning

On the 30th of May, a revisit of the building took place, with the primary objective being the photogrammetry process. To capture a comprehensive representation of the structure, a RICOH THETA 360 camera was employed. The selection of this particular camera model was based on its capability to capture high-resolution images in a 360-degree field of view, thereby enabling more immersive and detailed documentation of the building's physical attributes. In order to process the data that the camera collected the phone application of Matterport was used. The application has the ability to generate a digital twin of the building, enabling the creation of a virtual replica that closely mimics the physical structure.



Figure 5.1 - RICOH THETA 360



Figure 5.2 - The Matterport application

The whole process was completed within approximately two hours. The comprehensive scanning of the building's interior has been successfully completed, capturing intricate details, and providing a detailed representation of its internal structure. However, it is important to note that the exterior of the building lacks the same level of information. The insufficient height of the tripod used during the scanning process prevented the capture of the roof and other exterior elements. While a drone could be utilized as a solution to overcome this challenge and capture the exterior and roof with greater accuracy, access to a drone within the available resources and time constraints was not able.

## 5.2 The Result

The outcome of the scanning process is an interactive 3D model that facilitates user navigation through the various rooms within the building.



Figure 5.3 - Overview of the 3D Model

To enhance the user experience and provide comprehensive information on different types of decay observed, some additional features have been used. These include the inclusion of tags within the 3D model, accompanied by photographs that depict specific instances of decay and their corresponding locations. By integrating these tags and detailed photographs, users can identify and examine various decay patterns as they navigate through the 3D model. This contributes to the overall understanding and documentation of the decaying elements within the building, enabling an overall analysis of its condition and providing a valuable resource for later researchers as long as the owner of the building.

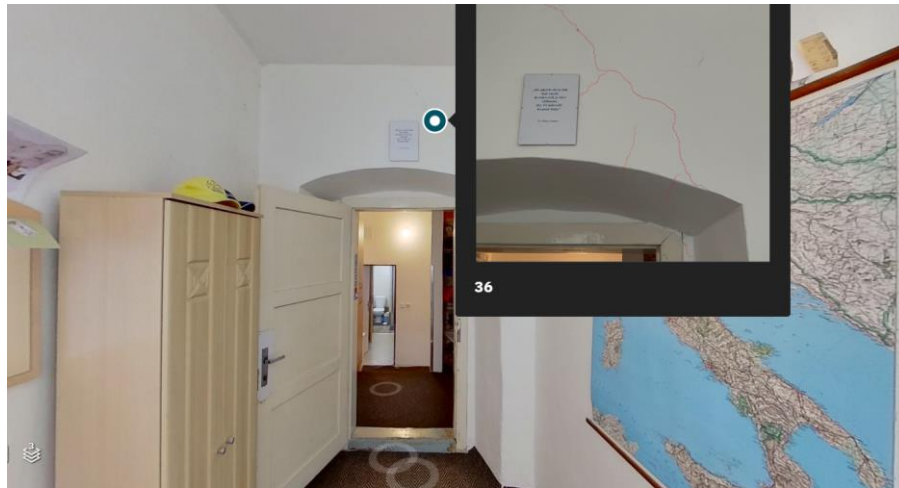


Figure 5.4 - Navigation in the interior and the additional tags for the decay

This page is left blank on purpose.

## 6. THE MODEL ANALYSIS

The absence of cracks in the exterior bearing walls indicates that the fractures observed in the interior are not a result of load-bearing capacity issues. As discussed in previous sections, the interior middle wall exhibits the most severe decay in the form of fractures, making it a focal point for modeling and static analysis. By selecting this wall for modeling, the intention is to accurately recreate its current condition and investigate whether ground deformations are the underlying cause of the fractures. Through the analysis, the structural response of the wall under the various loads and ground conditions can be accessed and thereby gain insights into the underlying causes of the decay.

### 6.1 Geometry

The geometry of the model was constructed using AutoCAD software, incorporating the information derived from existing drawings and the available 3D model of the building. To facilitate the transfer of the model into the ATENA software, which is utilized for static analysis, a simplification process was implemented. The overall thickness of the elements is 0.85 m. However, in order to take into consideration, the increased load-carrying capacity and stiffness of the bearing elements, those were modelled with a higher thickness than the rest. Figure 6.1 presents the thickness of the exterior walls that was taken into consideration.

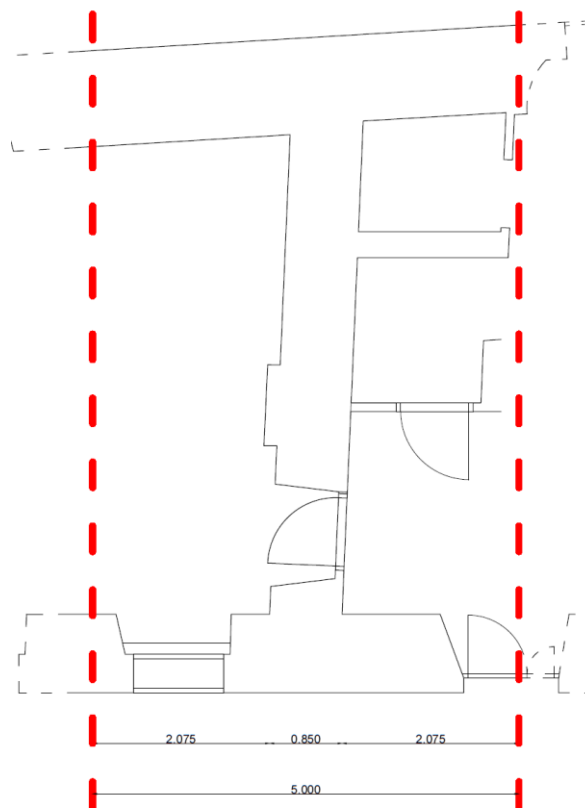


Figure 6.1 - Plan view of the wall and the total thickness of the exterior walls

The simplified geometry of the wall is presented below.

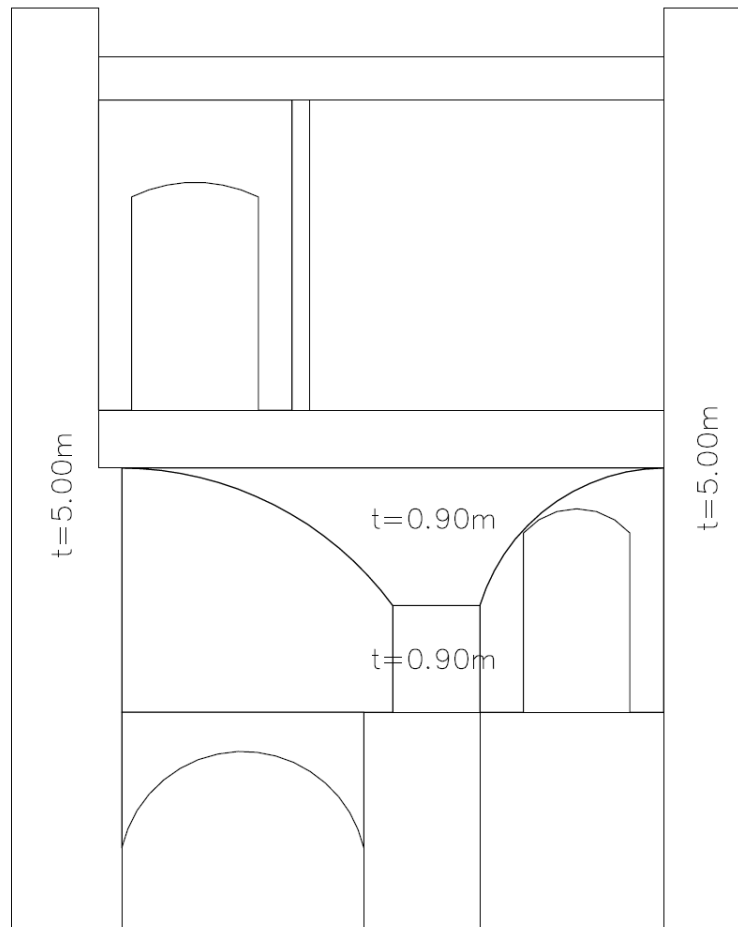


Figure 6.2 - Simplified geometry of the wall

## 6.2 Material Properties

The process of identifying material properties for existing structures has significant challenges. Since the building under study was constructed during a period without specific codes and regulations, the properties of the materials used are largely unknown. Therefore, non-destructive, and destructive tests are become necessary to gain insights into the material characteristics. However, due to limitations in resources and time, physical testing was not feasible within the scope of this thesis. Consequently, several material parameters were either assumed or calculated using the Masonry Quality Index (MQI) method, to assess the material properties and inform the subsequent analysis and modeling processes.

### 6.2.1 Masonry Quality Index

In the absence of detailed information regarding the specific materials of the construction of the building, a qualitative criterion, known as the Masonry Quality Index (MQI), was used to evaluate the quality of the units and mortar [24]. The MQI assesses whether a historic masonry wall was built according to the “rule of the art”, by identifying the presence of seven parameters:

- Conservation state and mechanical properties of the units (SM),
- Units dimension properties (SD),
- Units shape (SS),
- Wall leaf connections (WC),
- Horizontal bed joints characteristics (HJ),
- Vertical joints characteristics (VJ),
- Mortar mechanical properties (MM).

These parameters are categorized under three possible outcomes, Fulfilled (F), Partially Fulfilled (PF), and Not Fulfilled (NF). The resultant values can be correlated to estimate the elastic modulus, compressive and shear strength of the wall.

Due to the complete plaster coverage of the walls throughout the building, conducting the MQI was challenging. However, P. ThLic. Martin Lanži was able to provide some photographs of the building during the demolition of the newest section, revealing the exposed masonry that was used for the evaluation of the wall.



Figure 6.3 - Uncovered wall



The values obtained for the parameters are presented in Table 6.1 along with the final value of the MQI and the characterization of the wall in each direction. For the calculation of the MQI, the equation of **Borri, Corradi, and de Maria**<sup>2</sup> for non-squared block masonry was used. The mechanical properties were calculated using the formulas given by the Italian code (MIT 2019) and the results can be seen in Table 6.2

Table 6.1 – Masonry Quality Index

Direction	SM	SD	SS	WC	HJ	VJ	MM	m	MQI(v)	Category	Characterization
Vertical	1	0.5	1.5	1	1	0.5	0.5	1	5	A	Good behavior of masonry
In-plane	1	0.5	1	1	0.5	1	1	1	5	B	Behavior of average quality for the masonry
Out-of-plane	1	0.5	1	1.5	1	0.5	0.5	1	5	B	Behavior of average quality for the masonry

Table 6.2 – Mechanical Properties values

Vertical	$f_{min}$ (MPa)	$f_{mean}$ (MPa)	$f_{max}$ (MPa)	$E_{min}$ (MPa)	$E_{mean}$ (MPa)	$E_{max}$ (MPa)			
		2.77	3.59	4.54	1313.03	1594.64	1863.64		
In-plane	$T_{0min}$ (MPa)	$T_{0mean}$ (MPa)	$T_{0max}$ (MPa)	$fv_{0min}$ (MPa)	$fv_{0mean}$ (MPa)	$fv_{0max}$ (MPa)	$G_{min}$ (MPa)	$G_{mean}$ (MPa)	$G_{max}$ (MPa)
	0.05	0.07	0.09	0.13	0.19	0.25	409.62	515.23	604.48

It is important to acknowledge that the MQI method is inherently subjective, as its evaluation relies on the expertise and judgment of the engineer conducting the assessment. The results obtained may vary depending on the individual evaluator. This subjectivity introduces a degree of uncertainty and highlights the importance of combining the method with other types of non-destructive or minor destructive tests.

## 6.2.2 Material Properties for Modelling

The analysis of the wall was carried out using the ATENA 2D software. Since the software is developed for reinforced concrete structures, the modeling of the masonry should be careful. The material type that was chosen for the modeling of the masonry was “3D Nonlinear cementitious 2” (Cervenka & Jendele, 2021) [25], which is a type of fracture plastic constitutive model available in the software. This fracture-plastic model is based on the orthotropic smeared crack formulation and crack band model. It employs the Rankine failure criterion, exponential softening, and it can be used as rotated or fixed crack model. The hardening/softening plasticity model is based on the Menétrey - Willam failure surface. The model can be used to simulate concrete cracking, crushing under high confinement, and crack closure due to

<sup>2</sup> Borri, A., Corradi, M., & De Maria, A. (2020) [24].

crushing in other materials. Also, in this material model, tensile behavior is described by an exponential opening law (Figure 6.4) which requires to directly set the fracture energy in tension.

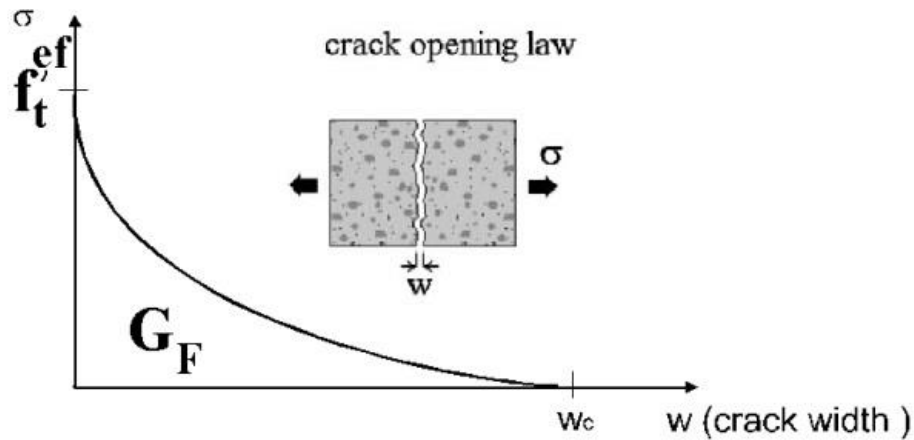


Figure 6.4 - Exponential crack opening law [25]

The material properties were defined mostly from the calculations of the MQI. For the compressive strength and the Young Modulus, the mean value was chosen. According to literature recommendations (Lourenço & Gaetani, 2022) [27] the value of the tensile strength can range between 3% to 10% of the compressive strength. For this model, the value was chosen as 5% of the compressive strength. Additionally, the tensile fracture energy is recommended to be taken as  $G_f = 0.05 \text{ N/mm}$  for masonry with good-quality mortar. The mechanical parameters and their values are listed in Table 6.3.

Table 6.3 – Material Properties for the Numerical Model

Material Properties	Values	Units
Youngs Modulus: E	1600	MPa
Poisson's Ratio: $\mu$	0.20	-
Mass Density: $\rho$	0.02	MN/m <sup>3</sup>
Tensile Strength: $f_t$	0.18	MPa
Tensile Fracture Energy: $G_f$	0.00005	MN/m
Compressive Strength: $f_c$	-3.59	MPa

Given the limited information and lack of details regarding the specific materials used in the construction of each individual wall, it was necessary to make certain assumptions in the modeling process. Therefore, in this thesis, all of the wall macroelements in the model were assumed to be constructed from the same material and possess identical material properties.

The absence of information regarding the construction of the walls is combined with the lack of data about the characteristics of the underlying ground, including its type, quality, foundation depth, and condition. Notably, the exterior left wall of the basement is constructed upon a section of the city wall,

which rests directly on the ground. In Figure 6.5 a view of the rear façade and the wall as it was decided to be modeled.

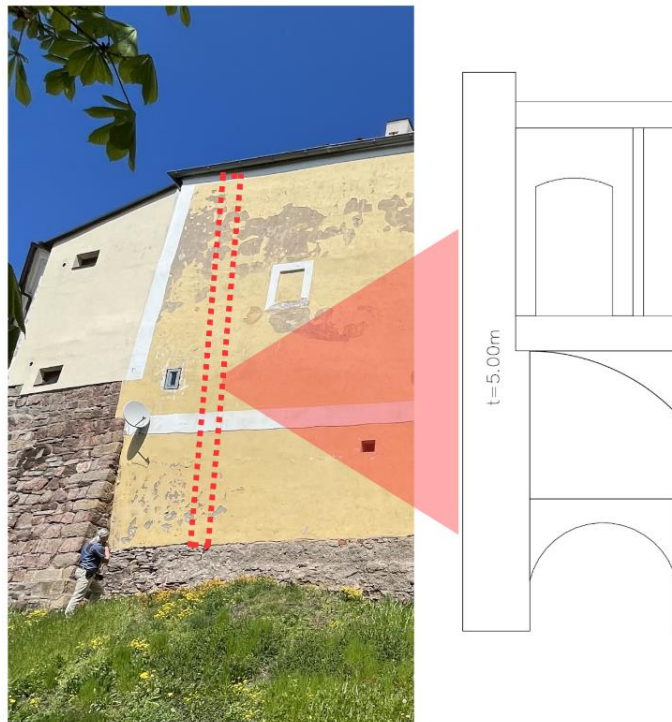


Figure 6.5 - View of the rear facade and the model of this part of the wall

Additionally, details regarding the section of the building adjacent to the basement remain unknown. As a result, it was presumed that this section is constructed from the same material as the rest of the building and extends to the same depth underground as the exterior left wall. Figure 6.6 presents the model of the basement, highlighted with red is the part of which the geometry is unknown.

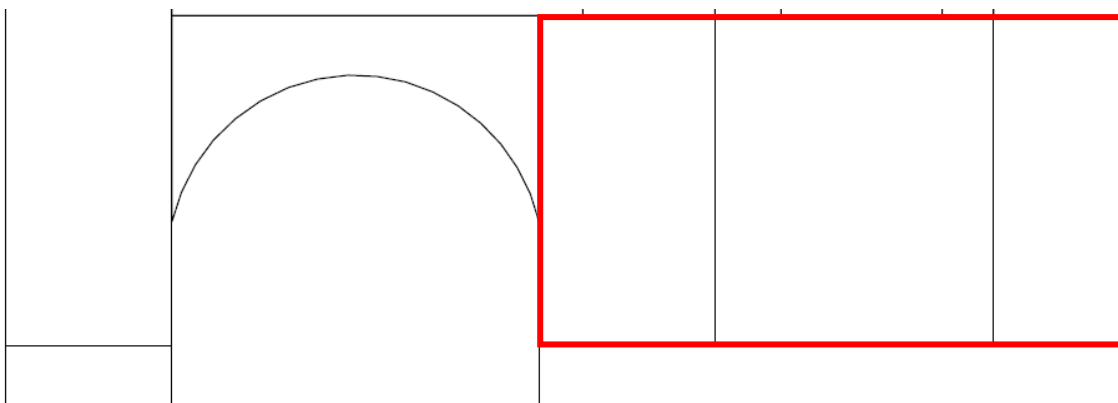


Figure 6.6 - The model of the basement

## 6.3 Current Loading Situation

### *Dead Load*

The dead loads of the structure are considered the self-weight of the masonry and the self-weight of the roof. The load attributed to the masonry was assigned in the software as the self-weight, with the density of the masonry material set at  $20 \text{ kN/m}^3$ .

A detailed calculation of the self-weight of the roof is presented in Annex paragraph 11.3. Considering the geometry described in paragraph 3.3 and the wood type assumed to be spruce for the parts of the truss and the roof battens, which has a density of  $3.7 \text{ kN/m}^3$ . The densities for the roof cover materials were obtained from the website of the company that supplies similar materials. According to the available information, the waterproof asphalt strip has a density of  $0.045 \text{ kN/m}^3$  [28]. As for the roof tiles the density of slate is  $26 \text{ kN/m}^3$ .

Considering the chosen thickness of the exterior wall and assuming that the modeled wall supports a timber truss, four trusses were found to transfer their load from the exterior walls of the model (Figure 6.7). The total load of these trusses is represented as a concentrated load positioned at the middle of the top of the exterior walls.

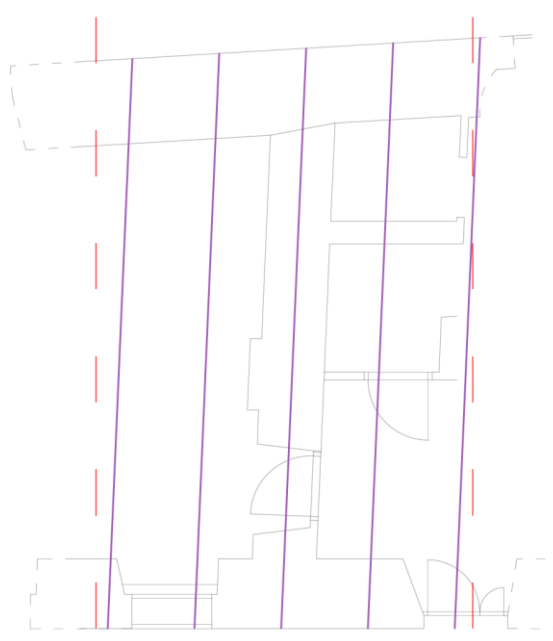


Figure 6.7 - Plan view of the wall with the trusses

Moreover, in addition to the previously discussed dead loads, the loads resulting from the presence of vaults attached to the wall were incorporated into the analysis (Figure 6.8). These loads consist of the self-weight of the vault structure and the floor that the vault supports above it (Figure 6.9). Each load is applied as a distributed load along the length of the wall where the vault is connected. The detailed calculation is presented in Annex paragraph 11.4.

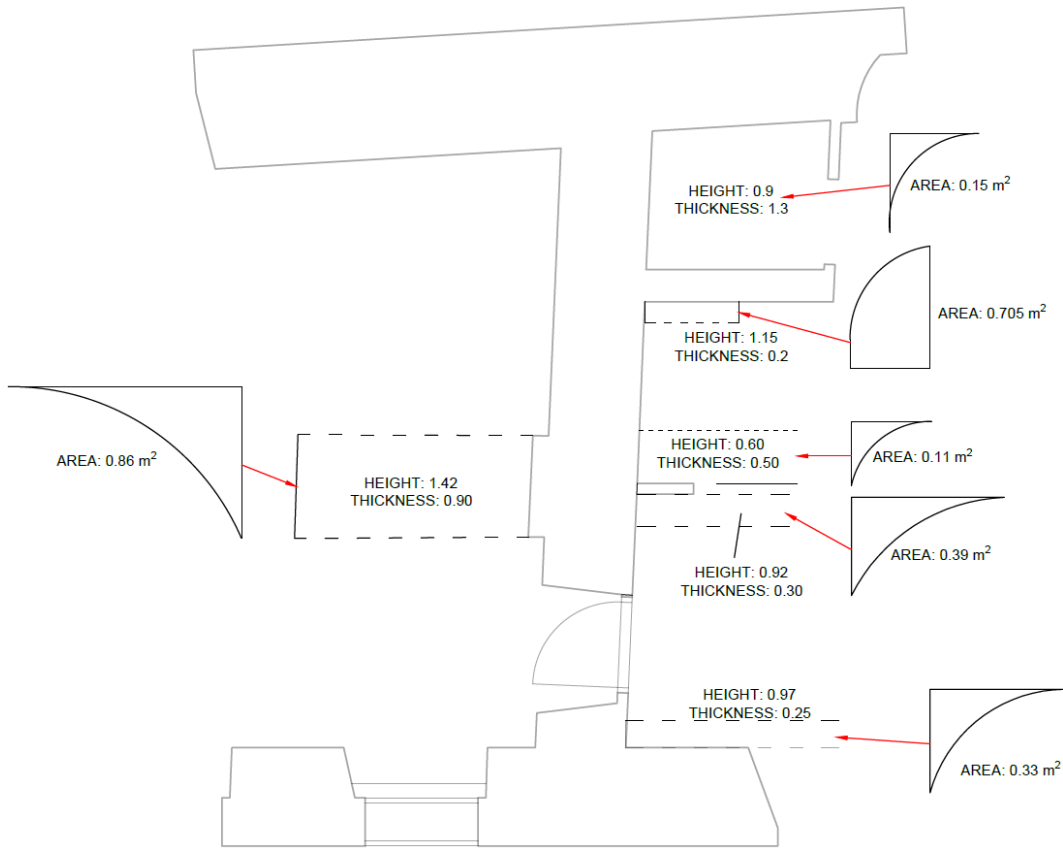


Figure 6.8 - Plan view of the vaults attached to the wall

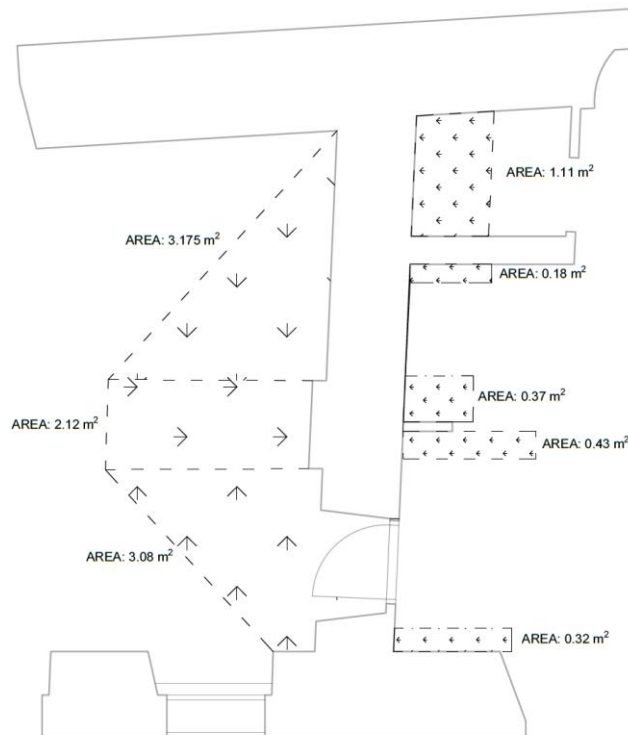


Figure 6.9 - The area of the floor supported by each vault

### Live Load

The live load of the structure consists of the live load of the floor of both floors, the live load of the roof, and the snow.

The live load of the floors is calculated according to EN 1991-1-1:2002 [29]. The category of the loaded area is Category A for which the imposed load is  $q_k=2.0 \text{ kN/m}^2$  (Figure 6.10). An additional  $0.5 \text{ kN/m}^2$  is added due to movable partitions having a total of  $2.5 \text{ kN/m}^2$  per floor. The load is modeled as a distributed load to the length of each floor.

Table 6.2 - Imposed loads on floors, balconies and stairs in buildings

Categories of loaded areas	$q_k$ [kN/m <sup>2</sup> ]	$Q_k$ [kN]
Category A - Floors	1,5 to 2,0	2,0 to 3,0

Figure 6.10 - Table 6.2 of the EN 1991-1-1:2002

As recommended by EN 1991-1-1:2002, roofs that are not accessible for anything other than normal maintenance and repair are subjected to a load of  $0.4 \text{ kN/m}^2$ . However, in accordance with table A1.1 of EN-1990 [30], when considering snow load, the combination factor for the roof live load is taken as 0.

For the Broumov region, the characteristic value of the snow load is determined to be  $2 \text{ kN/m}^2$ , following the recommendation of the Czech Republic National Annexes (Figure 6.11). The load is calculated for the area of the roof shown in Figure 6.7 and is modeled as a concentrated load at the same point as the dead load of the roof. The detailed calculation for the snow load is presented in Annex paragraph 11.5.

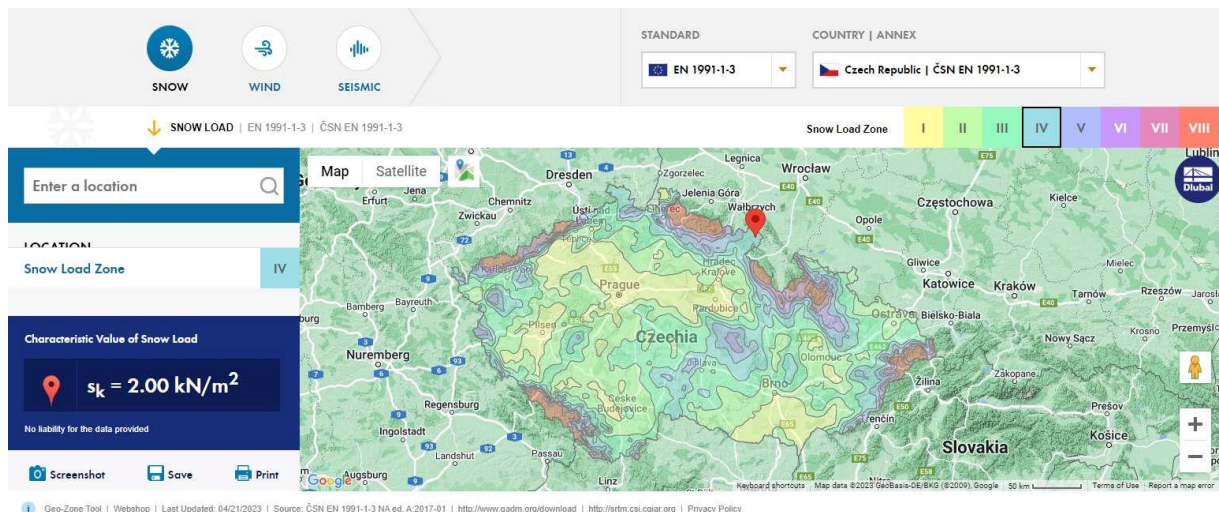


Figure 6.11 - Snow Load Map of the Czech Republic [31]



## 6.4 Boundary Conditions

In the main model, the boundary conditions were defined using springs with varying stiffness values along different sections of the base macro-elements. Since detailed information about the ground conditions was not available, the stiffness values for the springs were adopted from previous studies conducted on the Broumov group of churches.

Considering the current condition of the building, varying stiffness values were assigned to the springs at the base of its macro-element (Figure 6.13). The exterior wall on the left side, which relies on the city wall, is assumed to have a better foundation condition compared to the other walls. Hence, the springs at the base of this wall were given the highest stiffness value of 25 MPa. The remaining walls were assigned lower stiffness values to account for the assumption of poorer ground conditions, with the value being 12.5 MPa. Furthermore, given the observed settlement in the basement (Figure 6.12), the springs of the wall beside the basement were assigned the lowest stiffness value of 7 MPa. These chosen stiffness values aim to accurately reproduce the existing crack pattern evident in the building, as discussed in paragraph 4.2 of the thesis.



Figure 6.12 - The condition of the basement of the building

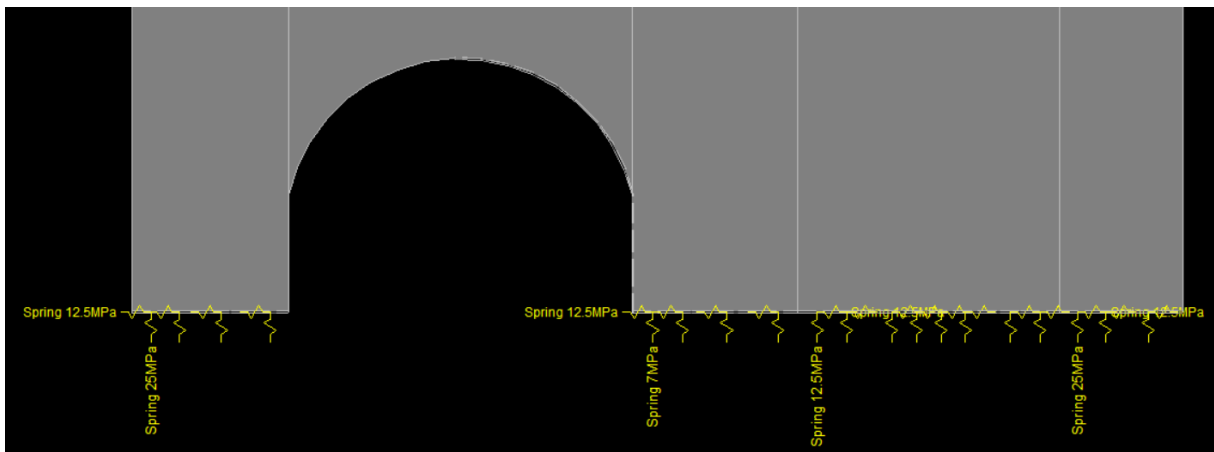


Figure 6.13 - The springs and their assigned values

## 6.5 Preliminary Analysis

The quality and size of the finite element mesh utilized in the analysis significantly impact the accuracy and reliability of the results. The selection of appropriate mesh size is crucial, as it can influence the bending behavior and overall stiffness of the structure. A mesh with large elements may restrict bending and result in a stiff representation of the structure. On the other hand, using a mesh with excessively small elements can lead to computational inefficiency without providing significant improvement in accuracy. For the analysis of this model, a mesh size of 0.20 m was chosen as an optimum compromise between computational efficiency and result accuracy.

The analysis of the model involved a step-by-step approach, where the loads applied on the building were gradually added in 10 analysis steps. The Newton-Raphson method was employed for the analysis of the model.

By dividing the analysis into multiple steps, the gradual application of loads allowed for a more realistic simulation of the structural response. Each step of the analysis involved updating the model's geometry and properties based on the current load state, thereby capturing the progressive behavior of the structure.

The choice of the Newton-Raphson method for the analysis was driven by its ability to handle the complexities associated with nonlinear structural behavior. This method provides reliable and accurate results, ensuring that the model's response to the applied loads is properly captured.

The crack pattern as a result of this analysis is presented in Figure 6.14.



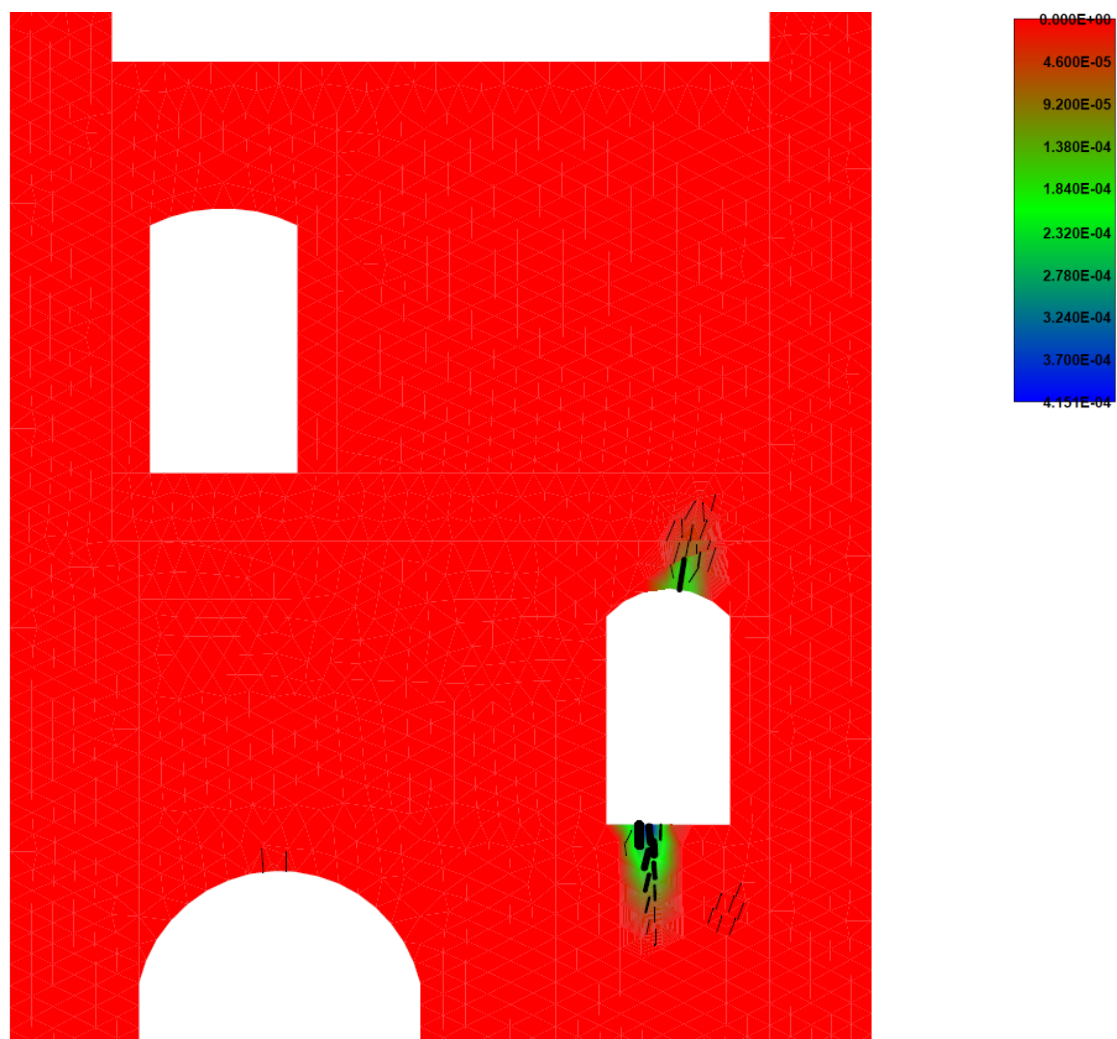


Figure 6.14 - Results of the preliminary analysis (m)

The analysis of the model did not reveal the exact crack pattern observed in the building. Moreover, the cracks that appeared were found to be minor. These findings indicate that the crack pattern observed on the walls of the building today cannot be attributed to a lack of bearing capacity, as the structure demonstrated sufficient strength to withstand the existing loads without any significant issues.

To ensure that the observed crack pattern is not created under the chosen circumstances, additional combinations of stiffnesses along the springs were tested. Approximately 30 different models were examined, considering variations in stiffness values, analysis methods (Newton-Raphson and Arc-length), and the number of analysis steps. However, these alterations did not result in any substantial differences compared to the results depicted in Figure 6.14.

In light of these findings, it became essential to examine alternative factors that may contribute to the observed crack pattern. Different scenarios related to the ground condition were investigated to determine their potential impact on the crack pattern. The models of these scenarios and their results will be discussed extensively in paragraph 6.6.

## 6.6 Analysis of Different Decay Hypothesis

Alternative scenarios were explored based on field observations and a static assessment conducted by ing. Jiří Švorc in January 2023 [32]. Two distinct cases were investigated to shed light on the potential causes of the crack pattern.

The first scenario draws from observations made by the thesis team during site visits. Clear evidence of settlement in various areas beneath the structure, particularly noticeable in the basement, supports this observation. This is further substantiated, as it was mentioned previously by the presence of cracks in both the church and the gymnasium, which are situated on the same cliff.

The second scenario aligns with Mr. Švorc's findings, suggesting that the foundation of the structure, particularly the city wall on which the left exterior wall is supported, is saturated with water. This water circulation within the porous materials leads to expansion when freezing occurs, thereby inducing the observed cracking pattern.

Both scenarios were examined using the same model as the preliminary analysis, with appropriate adjustments made to simulate the specific ground conditions associated with each scenario (Figure 6.15).

The ground itself was modeled as a plane stress elastic isotropic material, exhibiting a high elastic modulus to impart rigidity. To facilitate a more even distribution of load and stress between the ground material and the masonry walls, an interface was introduced at the base of the walls (Figure 6.16). This implementation acts as a buffer, mitigating the potential for localized stress concentrations and subsequent structural failures such as cracks or fractures. By incorporating this interface, the model aims to have a more realistic representation of the interaction between the building's walls and the underlying ground.

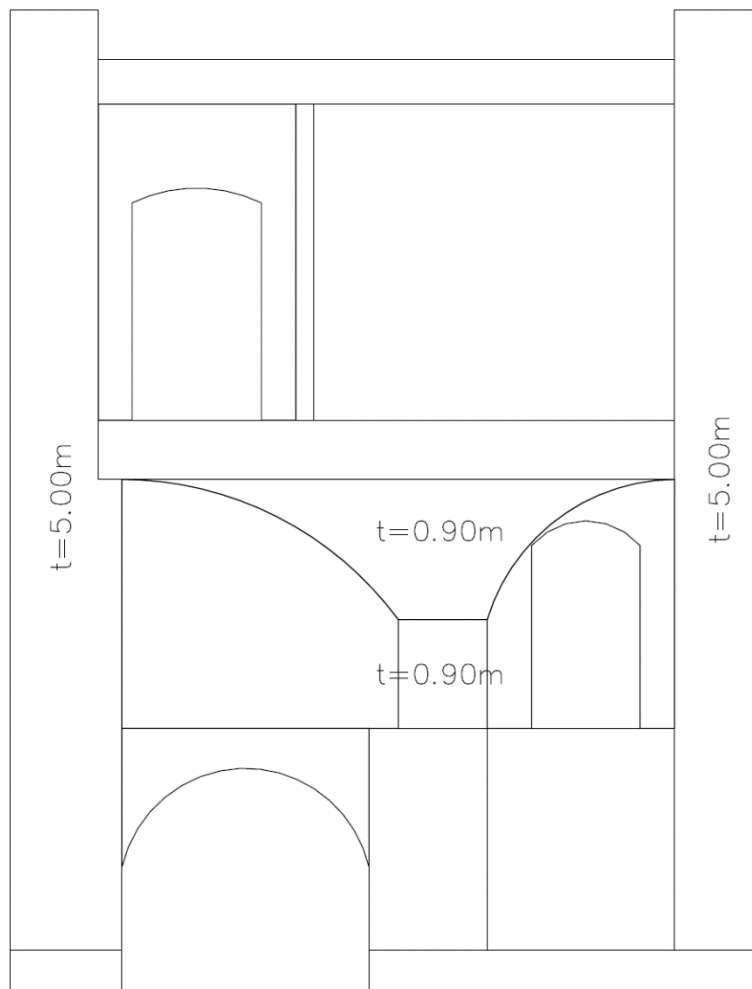


Figure 6.15 - The model with the ground modeled as a rigid material

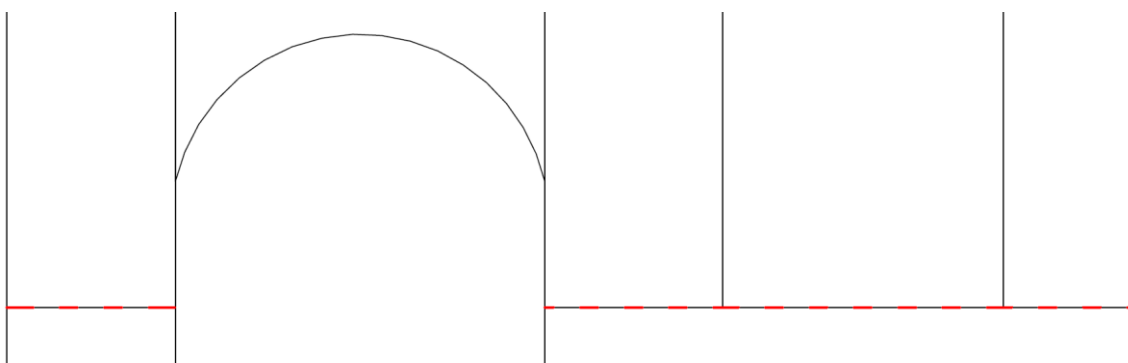


Figure 6.16 - The interface between the wall's base and the ground

The interface between the base of the walls and the ground was designed with specific stiffness properties to control its behavior. The normal stiffness was assigned a high value to prevent any significant deformation and ensure a rigid connection between the surfaces it joins. This decision aims to maintain the integrity of the interface and minimize the potential for displacement or separation

between the walls and the ground. The tangential stiffness of the interface was set to have a lower value to facilitate sliding or relative motion between the contacting surfaces. By allowing this relative motion, the model acknowledges the possibility of horizontal displacement or shearing forces that may arise due to ground movements. The properties of the interface are presented in Table 6.4.

Table 6.4 – Material properties for the Interface

Material Properties	Values	Units
Normal Stiffness: $K_{nn}$	40000	MN/m <sup>3</sup>
Tangential Stiffness: $K_{tt}$	10000	MN/m <sup>3</sup>
Tensile Strength: $f_t$	1	MPa
Cohesion: C	1	MPa
Friction coefficient	0.5	-

### 6.6.1 Ground Settlement

The analysis of the updated model is conducted in two parts. In the first part, similar to the preliminary analysis, the model is subjected to gradually increasing loading conditions in each step. The boundary condition is considered to be fixed (Figure 6.17).

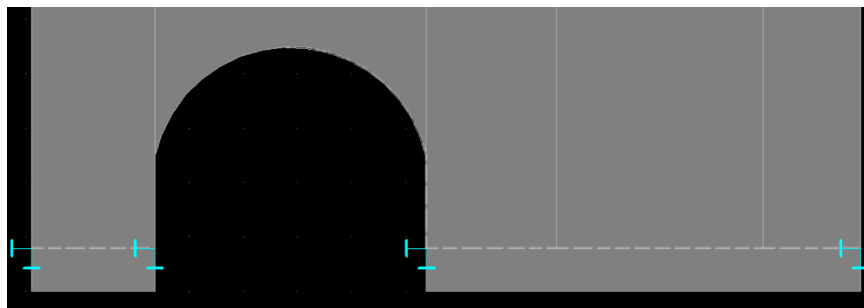


Figure 6.17 - The boundary condition for the first 10 steps of the analysis

After the initial 10 steps, the analysis shifts its focus to the displacement applied at the base of the elements (Figure 6.18). These displacement values are determined based on information gathered from previous theses conducted on the Broumov group of churches, which share geological characteristics similar to the present case study. The settlement of the ground in those theses ranged from approximately 1 cm to 2 cm. To evaluate the structure under the worst-case scenario, the highest displacement value is selected.

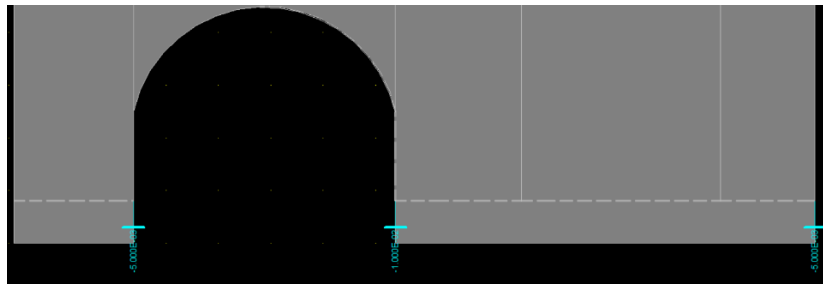


Figure 6.18 - The prescribed displacement at the base of the structure

The visual inspection indicates that the basement wall is likely to experience the most significant deformation. That combined with the direction and the shape of the cracking pattern suggests minor displacement in all the elements. To ensure a smooth settlement distribution across the baseline, a triangular shape is adopted, with the peak positioned beneath the basement wall.

The second part of the analysis is a combination of the Newton-Raphson and arc length methods, for 20 additional steps. The results of the analysis are presented in Figure 6.19

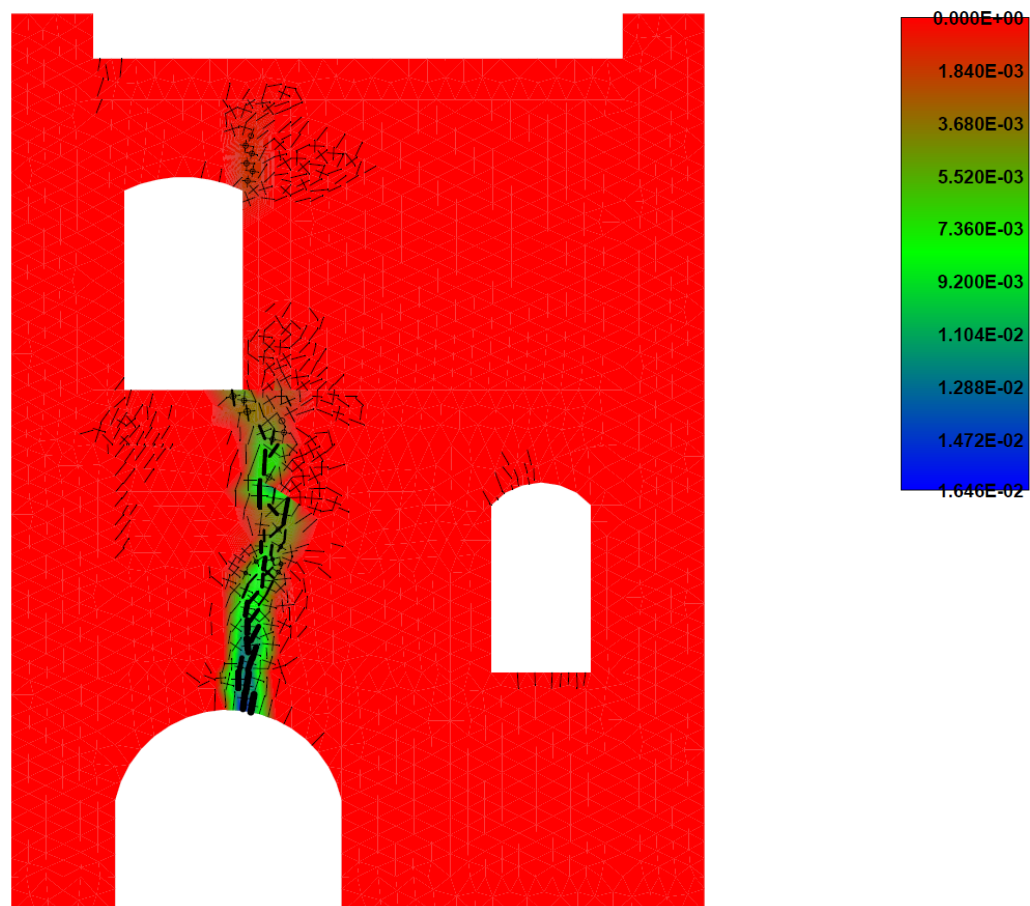


Figure 6.19 - Results of the settlement analysis (m)

Comparing the results of the analysis with the reality (Figure 6.20), some similarities can be observed. However, when taking into account the width of the cracks rather than solely focusing on their pattern, only the vertical crack above the basement vault exceeds a width of 1 cm. In contrast, the cracks around the door of the upper floor have widths of less than 1 mm. This indicates that if the situation were as depicted in the analysis, these cracks would likely not be visibly noticeable, which contradicts reality.

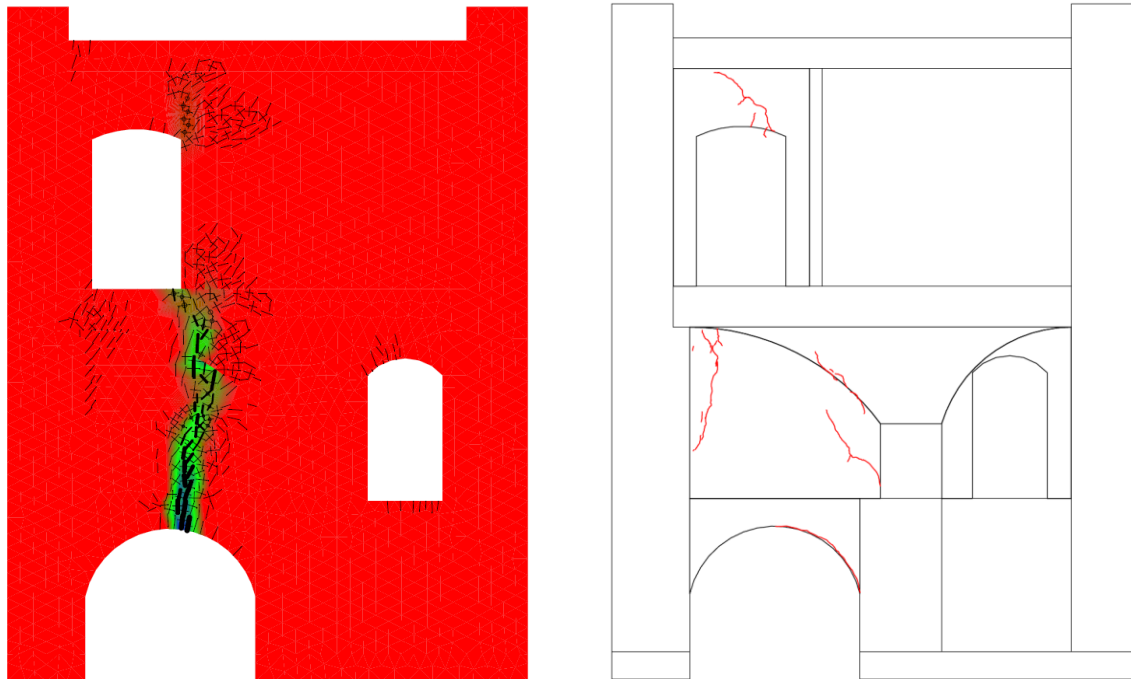


Figure 6.20 - Comparison between the analysis crack pattern and the expected one

### 6.6.2 Other settlement hypotheses

Two more hypotheses that were tested for this scenario and are worth mentioning are discussed below.

#### Settlement of the left wall

The first hypothesis tested is settlement to happen only on the exterior left wall. Since the wall is based on the city wall it was assumed that the wall might give in to the weight of the building and create settlement in horizontal and vertical direction as depicted in Figure 6.21.

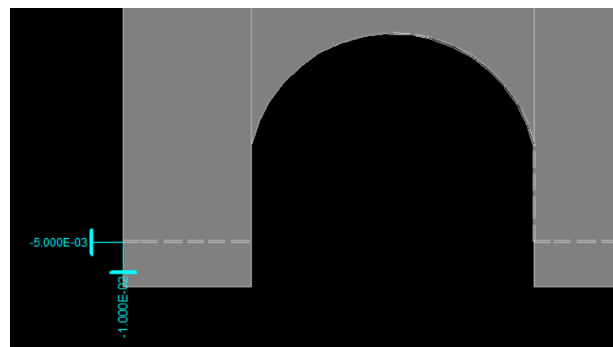


Figure 6.21 - The settlement of the left wall as prescribed displacement

The results of this analysis in comparison with reality are presented in Figure 6.20.

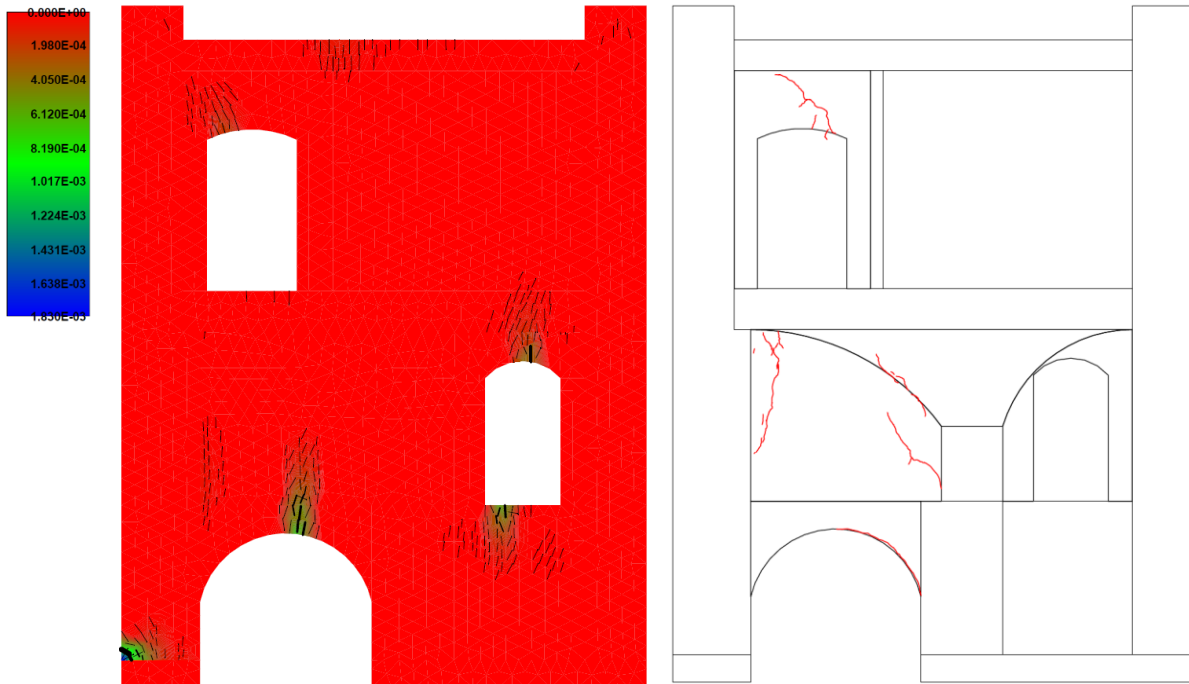


Figure 6.22 - Comparison between the analysis crack pattern and the expected one (m)

**Settlement of the right part of the building**

The second hypothesis tested is settlement to happen only on the right part of the building. The hypothesis was formulated based on the assumption that the ground beneath that particular section of the building has experienced greater settlement compared to the surrounding areas. Additionally, considering the absence of evident significant decay in the city wall, it is possible that the settlement issue is primarily concentrated beneath the building itself. The settlement selected as depicted in Figure 6.26.

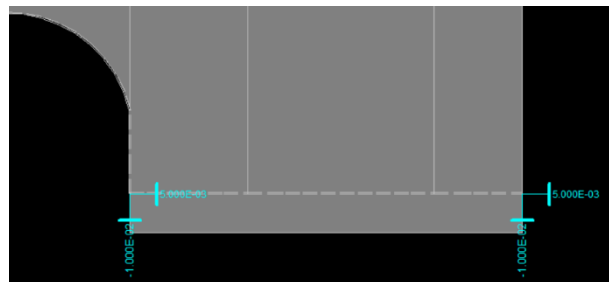


Figure 6.23 - The settlement as prescribed displacement

The results can be seen in Figure 6.24.

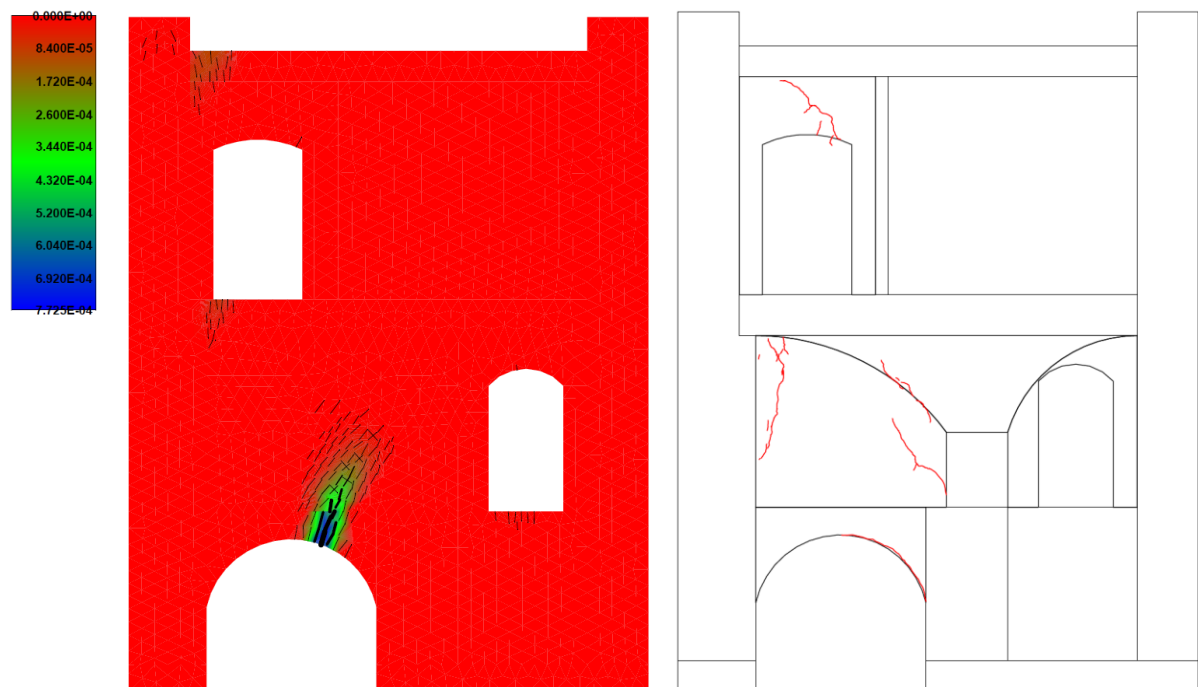


Figure 6.24 - Comparison between the analysis crack pattern and the expected one (m)

#### **Comment on the results of these two hypothesis**

Both of these analyses exhibit cracking patterns that do not align with the desired outcome. Additionally, the width of the cracks in both cases is considerably small. The direction and location of the primary cracks also differs from the intended objective. Consequently, it can be assumed that settlement has likely occurred along the entire length of the building's base rather than being concentrated in a single area.

### **6.6.3 Freezing-thaw Circle**

The freezing-thaw cycle has a significant impact on masonry walls, particularly in regions where temperatures can be below 0 °C for a long period of time, like Broumov. The process begins when water penetrates into the porous structure of the masonry. When this water freezes, it expands, exerting pressure on the surrounding materials. This expansion can cause micro-cracks or damage within the masonry. During the thawing phase, the ice melts and transforms back into water. However, the water may not always fully evaporate or drain out from the masonry, especially if the wall has limited permeability. As a result, the water can remain trapped within the masonry, leading to further deterioration. The repeated freezing and thawing cycles exacerbate the damage to the masonry wall. With each cycle, the cracks and gaps within the masonry widen, allowing more water to infiltrate.

Although the available data do not provide sufficient information about the saturation of the building's walls, Mr. Švorc's static assessment points to the freezing-thaw cycle as the likely cause of the cracks. As a result, this is a hypothesis that requires further testing and investigation to confirm.



Determining the appropriate displacement value to simulate the expansion of the wall due to the freezing-thaw cycle was a challenging task. Due to the lack of data on parameters such as wall and foundation saturation, masonry porosity, mechanical properties of the foundation, and soil characteristics, the assumption was made based on a worst-case scenario. This approach accounts for the highest potential displacement and the cracking pattern that it creates.

Similar to the settlement model, the analysis, in this case, is divided into two stages. The first stage involves the gradual application of load over the course of 10 steps, with a fixed boundary condition. In the second stage, displacement is introduced to the building. It is assumed that the exterior wall, which is built on the city wall, is the most susceptible to displacement. This assumption is based on the fact that the city wall is exposed to atmospheric conditions, making it more vulnerable to water infiltration and as a result to be affected by the freeze-thaw cycle.

The chosen displacement to represent the expansion caused by water freezing is 1 cm (Figure 6.25). Considering that water expands by approximately 9% when frozen, it implies that for the city wall and its underlying foundation, if they exist, to experience such a displacement, they will need to have a significant degree of porosity and be fully saturated with water [33]. This would allow the frozen water to create high pressure on the elements of the masonry, resulting in the expansion of the wall, which creates upward movement of the building.

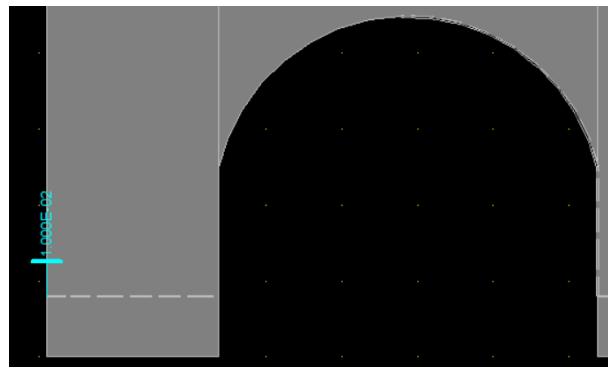


Figure 6.25 - The upward displacement of the left exterior wall

The results of the analysis are presented in Figure 6.26

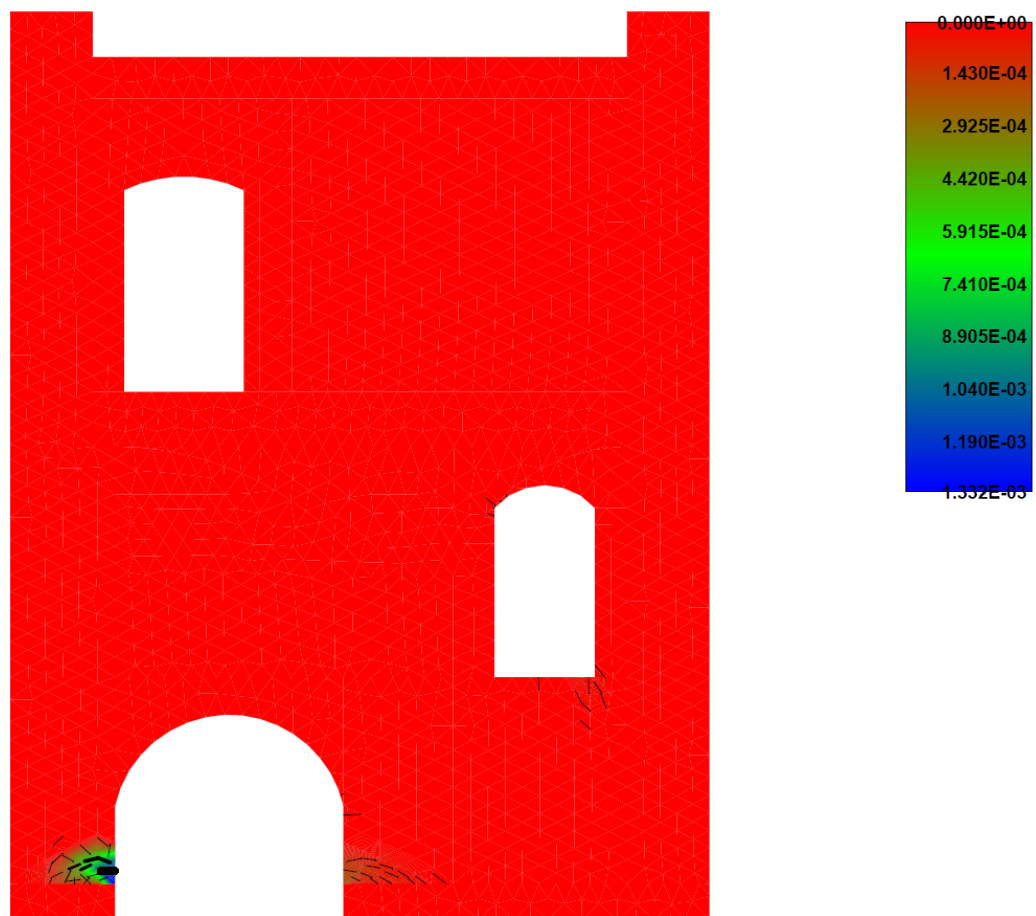


Figure 6.26 - Results of the settlement analysis (m)

Comparing the results of the analysis as before (Figure 6.27), it becomes evident that the crack pattern observed does not align with reality. However, it is important to consider that the assumptions made during the modeling process may have influenced these outcomes. The results could be significantly different if the actual process and real data were utilized in the analysis.

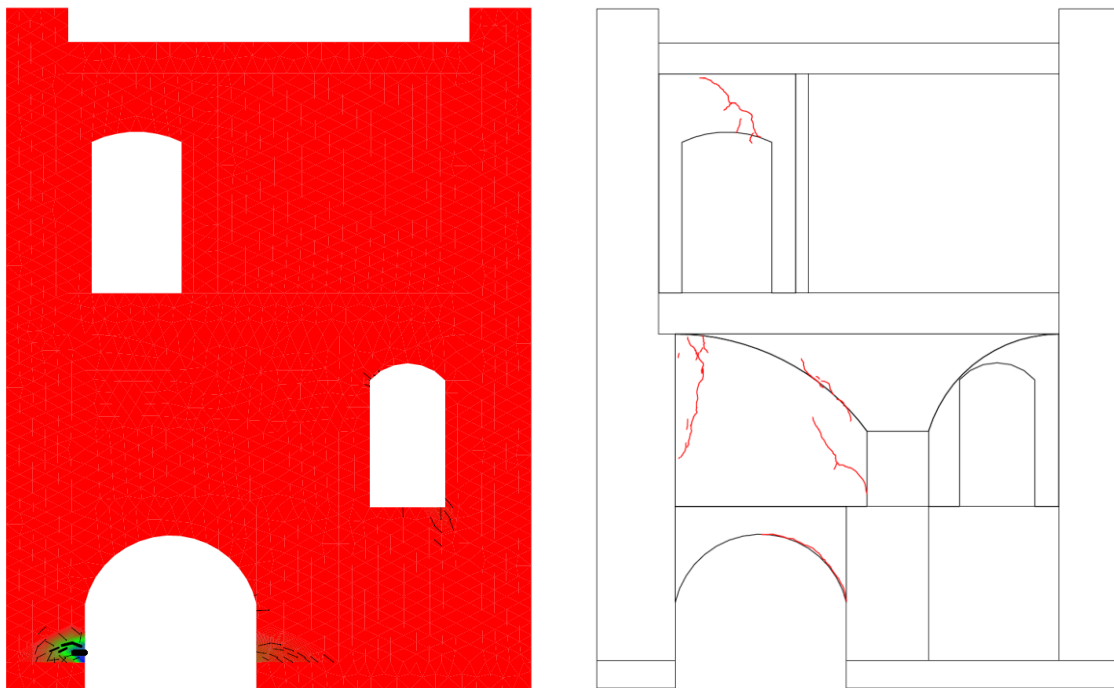


Figure 6.27 - Comparison between the analysis crack pattern and the expected one (m)

#### 6.6.4 Other freeze-thaw circle hypotheses

As for the settlement, some more hypotheses were tested for the scenario of expansion due to freeze-thaw circle phenomenon and are worth mentioning are discussed below.

##### Expansion of both exterior walls

An alternative hypothesis for this scenario is that both exterior walls undergo displacement caused by the freezing-thawing cycle. Considering that the foundation beneath the right wall does not directly interact with the environment, unlike the city wall beneath the left wall, it was assumed that the displacement beneath the right wall would be comparatively smaller. The chosen displacement for testing purposes is illustrated in Figure 6.28.

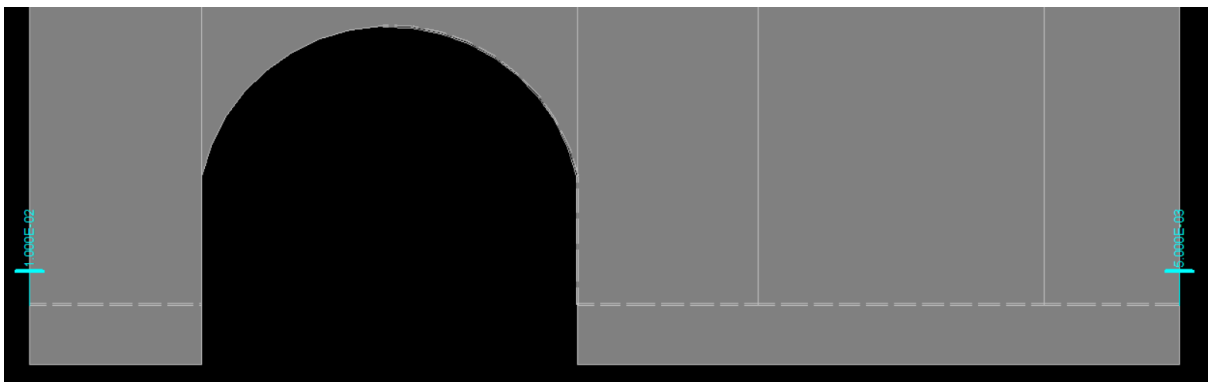


Figure 6.28 - The settlement of the right part as prescribed displacement

The results of this analysis in comparison with reality are presented in Figure 6.29.

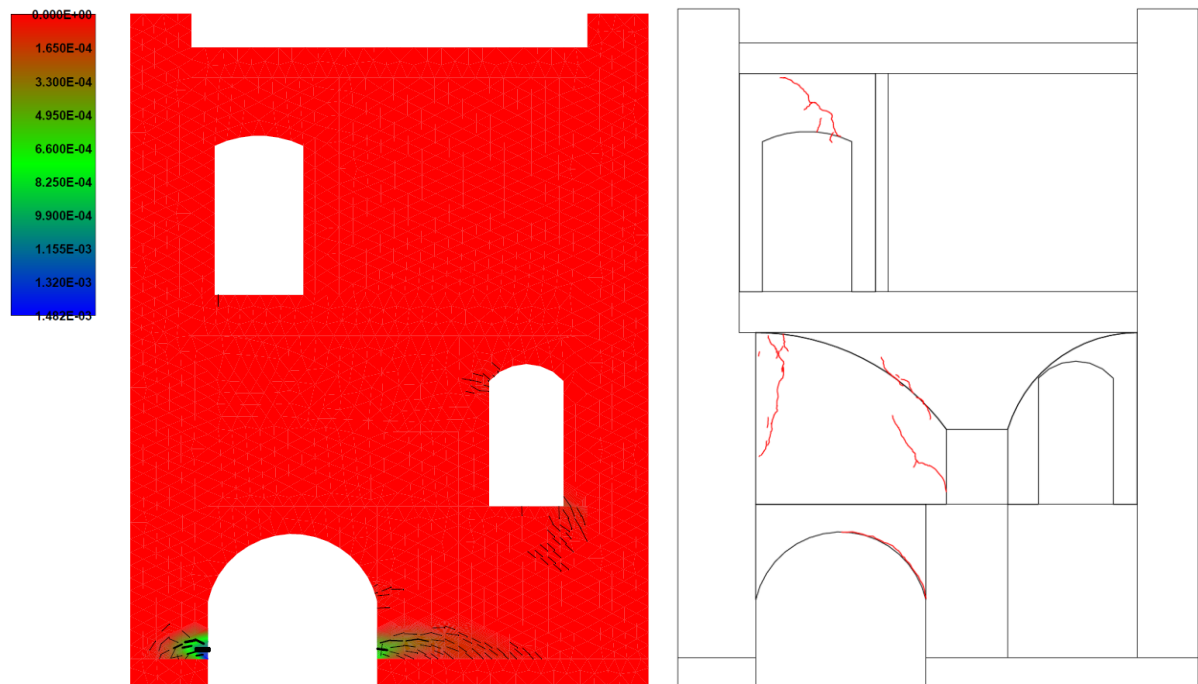


Figure 6.29 - Comparison between the analysis crack pattern and the expected one (m)

The obtained result aligns closely with the original hypothesis, with minimal deviation. However, the observed crack pattern does not match the actual reality. It is important to emphasize that all the assumptions made during the analysis are approximate, and it is highly likely that the results could significantly differ if the data were the real ones.

### 6.6.5 Other types of models tested

#### The primer model

Except from the models mentioned above, more scenarios were tested in order to extract the wanted result. The initial model that was created had slight differences compared to the final model used, as depicted in the figure below (Figure 6.30).

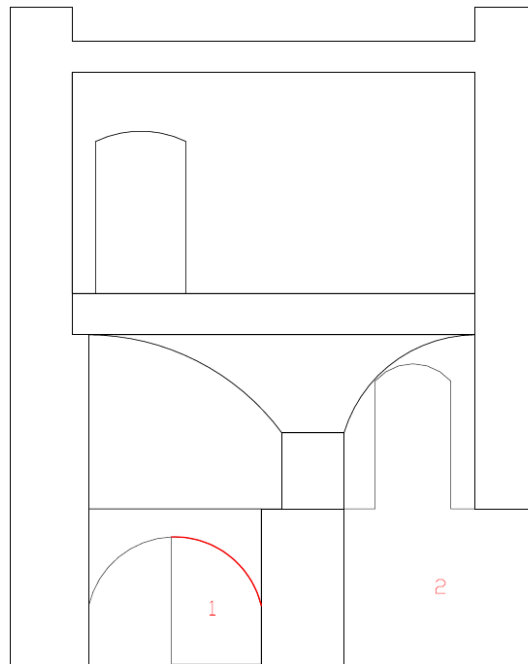


Figure 6.30 - The first model

The key differences in the final chosen model are as follows: Firstly, the wall that became detached at the basement is modeled with an interface separating it from the arch above (referred to as no. 1 in Figure 6.30). Secondly, the macroelements below the right part of the wall are not included in this model due to a lack of information regarding that specific area (referred to as no. 2 in Figure 6.30). Finally all of the macro-elements in this model have the same thickness and the same material properties.

All of the various scenarios discussed previously (spring boundary conditions, settlement, freezing-thaw cycle) were also tested for this model. However, several challenges were encountered during each analysis. Primarily, many of the analyses could not be completed due to convergence issues. Moreover, in order to achieve the desired cracking pattern or make the model run, certain assumptions had to be made that may not reflect in reality conditions. After multiple attempts, it was concluded that the detached basement wall should be removed from the model. Additionally, considering the right part's exterior wall acts as a bearing wall, it was determined that it should extend to a greater depth than just the surface of the ground. Consequently, the model was modified to the version discussed in paragraph 6.1.

### **Model without solid macro-elements for the ground**

All scenarios were also tested in a model where the ground was not represented as a solid macro-element. In this model, the initial boundary conditions were fixed supports, with the load gradually applied for the first steps of analysis and then displacement introduced to the building in specific elements while keeping the uninvolved parts fixed. An example of such an analysis can be seen in Figure 6.31.

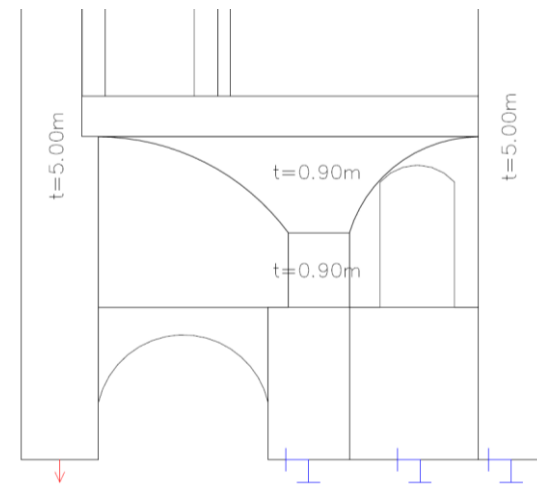


Figure 6.31 - Settlement analysis with fixed boundary conditions

The problem with this models was that its displacement had to be modelled evenly in the whole length of the element. However, by neglecting the ground's solid representation, the models failed to account for differential settlements. This oversight leads to an uneven distribution of stresses, which, in turn, caused convergence issues.

## **6.7 Conclusion of the Model Analysis**

Unfortunately, within the scope of this thesis, it was not feasible to gather the necessary data required for creating a model that closely represents the reality of the situation. Consequently, none of the tested models produced the crack pattern observed in the structure. It is important to emphasize that the models presented in the paragraph were selected after numerous attempts, combinations, and assumptions. Approximately 100 different models were analyzed, revealing the significant challenge of simulating reality without proper testing and data collection.

However, it is worth noting that the settlement analysis model demonstrated promising results. This suggests that, when combined with real data or other pertinent factors, this model has the potential to produce a more accurate representation of the actual crack pattern.

This page is left blank on purpose.

## 7. CONSIDERATIONS FOR AN ACCURATE MODEL

Upon the various model analysis, it became evident that recreating reality was a challenging task given the limited data available. Unfortunately, due to constraints during the thesis, critical testing and investigation phases were prevented, resulting in less accurate results that deviated from real conditions.

The models that were created for the thesis presumed a homogenized composition of the masonry, assuming uniform properties across different elements. Additionally, since no information was accessible regarding the ground's characteristics, such as its morphology and quality, or details about the foundations including their length and condition, all assumptions made may significantly diverge from actual conditions.

For the model to be more accurate and simulate reality better some specific tests and procedures should be followed.

In order to obtain a comprehensive understanding of the structure, a more thorough investigation of its historical background is essential. The currently available data are insufficient, particularly regarding the materials used and construction techniques employed. Obtaining detailed knowledge of the chronological sequence of construction and the order in which different parts of the building were built is crucial for comprehending the load transfer mechanisms within the structure. For instance, it would be valuable to determine if the detached wall was constructed before or after the rest of the vaulted basement. Furthermore, additional information is needed to have information about the part on the right side of the basement.

It is also important to conduct a more comprehensive examination of the building's geometry. The existing drawings are inadequate and lack crucial details. While the 3D model created is suitable for preliminary evaluation, it should be complemented with other methods. For example, using a laser meter to measure specific dimensions, especially the height of each room, is necessary. The exterior of the building, which was not adequately scanned, as it was mentioned previously, must be captured to enable future condition comparisons. Additionally, the accuracy of the structural heights as depicted in the existing drawings needs to be verified. Finally, the exact geometry of the roof is important to be investigated.

To ascertain the properties and characteristics of the materials used, it is recommended to conduct non-destructive and minor destructive tests [34]. Samples of the masonry employed in the construction should be collected, and laboratory tests should be performed to determine its composition, strength, porosity, and other relevant properties. These analyses will provide precise insights into the material's characteristics and help refine the assumptions made in the models. If collecting material samples is not feasible, conducting a Schmitt hammer test becomes crucial in order to gather information about the mechanical properties of the masonry walls. Sonic and ultrasonic testing should also be employed to assess the internal structure of the masonry walls without causing damage. These methods can reveal



vital information about the presence of voids, cracks, or other defects that may impact the structural integrity of the building.

Furthermore, conducting an endoscope test on the cracks, particularly in the basement area, would be a valuable solution. The endoscope test can provide important insights into the nature and severity of the cracks, such as their width, depth, and any potential signs of displacement or deterioration. This information is crucial for understanding structural behavior and identifying any potential risks associated with the cracks.

Certainly, gathering information about the underground conditions of the building is crucial, especially in cases like this one where there are indications of issues affecting the structure [35]. Understanding the characteristics of the soil, groundwater levels, and geological deformations that might exist can define the correct cause of the crack patterns in the building. It is important to perform comprehensive ground testing and site characterization to understand the properties and behavior of the soil or rock underlying the building. This typically involves conducting geotechnical investigations, including soil sampling, laboratory testing, and in-situ testing methods such as cone penetration tests (CPT) or standard penetration tests (SPT). These tests help determine soil composition, strength, bearing capacity, settlement characteristics, and other relevant geotechnical parameters. Ground-penetrating radar (GPR) is also a commonly used technique in soil monitoring and investigation. It can provide information about the depth and thickness of different soil layers. By analyzing the reflected radar waves, it is possible to identify variations in soil properties, detect layer interfaces, such as changes in soil composition or the presence of groundwater, and identify voids, cavities, and other anomalies within the soil. Furthermore, understanding the groundwater conditions is vital for assessing their impact on the foundation and overall stability of the structure. Monitoring groundwater levels and conducting hydrogeological studies can provide insights into water table fluctuations, seasonal variations, and potential water-related issues, such as soil erosion or excessive pore water pressures. Finally, an investigation of the building's foundation is crucial to assess its condition, adequacy, and compatibility with the underlying ground conditions.

## 8. CONCLUSION

In conclusion, this thesis has focused on evaluating the condition of the parish house and investigating its deterioration. The initial phase involved understanding the building's history, and geometry, and evaluating the severity of various decay issues. The most significant concern was the presence of structural cracks surrounding the middle wall, which became the primary focus of the study.

Unfortunately, due to constraints and limitations, obtaining crucial data regarding material properties, soil characteristics, and sub-surface building geometry was not feasible. As a result, all the analyzed models were based on assumptions.

Despite the challenges posed by the lack of specific information, numerous models were examined to explore different scenarios concerning the causes of the cracks. Although representing the crack pattern accurately proved to be unattainable, the settlement analysis model demonstrated promising results. Nonetheless, the analysis indicated that the building has adequate bearing capacity, as it effectively withstands the imposed loads without issues.

Additionally, the utilization of the 3D model generated through photogrammetric methods emerged as a valuable tool for ongoing crack monitoring and future comparisons of the building's condition.

It is important to acknowledge that further testing and data collection are imperative to enhance the understanding and modeling accuracy of the building's behavior. Future research should focus on obtaining comprehensive information regarding material properties, soil characteristics, and sub-surface geometry to refine the modeling approach and gain a more comprehensive understanding of the deterioration mechanisms.

Moreover, it is crucial to take into account the deterioration, and a more detailed study of specific parts of the building is also considered important. Detailed suggestions and recommendations regarding the monitoring and study of specific aspects of the building can be found in paragraph 9 of the thesis.

In summary, it is really important to highlight the significance of maintaining historical buildings, particularly those housing precious treasures like the frescoes in the parish house, which have survived since the 14th century. Despite the neglect suffered by both the frescoes and the building until recent years, this thesis lays the foundation for a more promising future, one centered around preservation and maintenance.

This page is left blank on purpose.

## 9. RECOMMENDATIONS

Chapter 7 discussed the significance of conducting multiple testing procedures to ascertain the characteristics of both the structural materials and the underlying soil. The present chapter aims to provide recommendations about the monitoring of various forms of deterioration observed in the building, along with proposing interventions and solutions to improve or maintain the structure's performance.

### **Crack and soil monitoring**

After conducting a visual inspection of the cracks and recording their location and extent, a start for monitoring these cracks has been established. Various options are available for monitoring crack behavior, depending on the level of precision and equipment cost.

One option is the installation of mechanical crack gauges or cracks meters across the main cracks. These gauges measure the width of the cracks and can track their eventual extension over time. Another option, somehow more expensive, is the use of electronic crack monitors equipped with sensors. These monitors can detect crack displacement or movement and provide continuous measurements of crack opening, closing, or stabilization.

In addition, to crack monitoring, more detailed photogrammetric scanning dedicated to capturing the cracking patterns of the building can offer more detailed information. This technique can be employed for monitoring purposes and serves as a reference for future comparisons, aiding in the assessment of crack progression.

As emphasized earlier, gathering information about the soil condition is crucial for ensuring the structural stability of the building. While determining mechanical parameters is important for the accuracy of the static model, monitoring events occurring beneath the ground is equally essential. Inclinometers can be used to measure horizontal and vertical soil movements or deformations. For precise monitoring of vertical soil settlement, settlement plates can be installed. These plates, measure periodically using surveying techniques, provide valuable insights into the long-term settlement behavior of the soil.

Another instrument of interest is the strain gauge, which monitors stress and deformation patterns within the soil or structural elements like foundations. By strategically placing these instruments within the building and the ground, the collected data can yield accurate and useful results for comprehensive monitoring of the structure.

By strategically placing these instruments and practicing the different proposed methods within the building and the ground, the monitoring results will be reliable, and relevant in understanding the behavior of the structure and its underlying soil. This informed data will facilitate effective decision-making processes and enable appropriate actions to maintain the stability and performance of the building.

### **Moisture detection and evaluation**

As highlighted in paragraph 4.2 the presence of moisture, particularly on the upper floor of the building, is of significant concern. Therefore, it is imperative to accurately detect and evaluate the extent and location of moisture.

One effective method for moisture detection is the utilization of thermal cameras. Thermal cameras detect thermal patterns and temperature variations on the surface of materials, enabling the identification of areas with potential moisture intrusion. Moisture typically exhibits a different thermal behavior than dry materials, making it distinguishable through thermal imaging.

### **Roof's condition evaluation**

Given that roof-related issues are suspected as the cause of the moisture infiltration on the upper floor, a thorough examination of the roof becomes crucial. Although from the exterior the condition of the roof seems to be good, a visual inspection from the interior can help identify visible signs of damage, deterioration, or inadequate sealing that could be contributing to moisture intrusion. The performance of leak tests can help identify areas where water penetration might occur. Also, since the roof is assumed to be constructed from timber some of the main elements should be tested to ensure the stability of the structure.

### **Further investigation of the fresco's room condition**

Although the thesis primarily focused on the cracking pattern of the middle wall, it is important to conduct further investigation in the fresco room. Despite recent studies and restoration work on the frescos, a more detailed examination of the entire space is necessary. The room was previously used as a chanel, and it is assumed that the ground level was lower during that time. Therefore, an investigation should be conducted to assess the condition of the ground beneath the room.

Additionally, cracks that are present on the ceiling and corners of the room require further investigation. These cracks may indicate underlying structural issues that need to be addressed. Furthermore, considering the moisture-related problems observed in other parts of the building, it is crucial to thoroughly test the fresco room for moisture. Moisture can have detrimental effects on frescos, potentially leading to their deterioration. Therefore, comprehensive testing and evaluation of moisture levels within the room are recommended to ensure the preservation of the frescos.

### **Re-plastering of the exterior walls**

One of the immediate actions that can be undertaken promptly is the repair of the exterior wall plaster. The investigation that took place during the first visit to the building indicates that the plaster on the exterior walls has experienced detachment, extensive blistering, and cracking (Paragraph 4.1). It is important to note that the plaster serves as a protective layer for the underlying masonry structure. Any further deterioration of the plaster could potentially lead to decay and damage to the masonry itself, as it becomes increasingly exposed to atmospheric conditions.

To prevent this situation, it is recommended to proceed with re-plastering work, employing lime plaster with a low strength but compatible with the materials comprising the masonry. Lime plaster is often preferred for its breathable properties and compatibility with historic structures. It allows for the diffusion of moisture and minimizes the risk of trapping moisture within the walls, thus reducing the likelihood of further damage.

This page is left blank on purpose.

## 10. REFERENCES

- [1] "Old Photo of Broumov." Fotohistorie. Accessed April 2023. Published on January 31, 2012. <http://fotohistorie.cz/Kralovehradecky/Nachod/Broumov/Default.aspx>
- [2] Czechia, Discover. 2019. A Brief History of the Czech Republic. August 31. Accessed April 2023. <https://www.czechuniversities.com/article/a-brief-history-of-the-czech-republic>.
- [3] Wikipedia. 2011. Czech Rep. - Bohemia, Moravia and Silesia III (en).png. August 07. Accessed April 2023. [https://commons.wikimedia.org/wiki/File:Czech\\_Rep.\\_-\\_Bohemia,\\_Moravia\\_and\\_Silesia\\_III\\_\(en\).png](https://commons.wikimedia.org/wiki/File:Czech_Rep._-_Bohemia,_Moravia_and_Silesia_III_(en).png).
- [4] Euratlas. 'Bohemia-Hungary in 1500.' Euratlas-Nüssli. 2009. Accessed April 2023. [https://www.euratlas.net/history/europe/1500/entity\\_35.html](https://www.euratlas.net/history/europe/1500/entity_35.html).
- [5] The Editors of Encyclopaedia Britannica. "Bohemia historical region, Europe." In Britannica. Last modified May 10, 2023. Accessed June 28, 2023. <https://www.britannica.com/summary/Bohemia>
- [6] <http://www.historyworld.net/wrldhis/PlainTextHistories.asp?groupid=2617&HistoryID=ac40&qtrack=pthc>
- [7] Vlach, Pavel. "Klášter Broumov - Broumov Monastery." Photograph. April 13, 2018. Wikimedia Commons. Accessed April 2023. [https://commons.wikimedia.org/wiki/File:Kl%C3%A1%C5%A1ter\\_Broumov\\_\(5\).jpg](https://commons.wikimedia.org/wiki/File:Kl%C3%A1%C5%A1ter_Broumov_(5).jpg)
- [8] Ptáček, Josef. "Stone Gate in the Broumovské Walls." Photograph. Accessed April 2023. From the project "Cultural and natural heritage for the Development of the Polish-Czech Borderland Common Heritage, reg. no. CZ.11.2.45/0.0/0.0/16\_021/0000760," Programme 2014 - 2020 INTERREG V-A Czech Republic - Poland. <https://www.hkregion.cz/redakce/index.php?dr=101051&lanG=cs&show=diskuze&>
- [9] Broumov, Městský úřad. 2012. Město Broumov. April 19. Accessed April 2023. <https://www.broumov-mesto.cz/vismo/dokumenty2.asp?id=1015&n=broumov%2Da%2Dokoli&defpc=1>.
- [10] Czech Geological Survey. "Geovědní mapy 1 : 50 000." Accessed April 2023. <https://mapy.geology.cz/geocr50/>
- [11] Climate-Data.org. Accessed April 2023. <https://en.climate-data.org/europe/czech-republic/broumov/broumov-58360/>
- [12] Team, Weather Spark. n.d. Weather Spark. Accessed April 2023. <https://weatherspark.com/y/81620/Average-Weather-in-Broumov-Czechia-Year-Round>.
- [13] Peterson, Adam. "Köppen climate types of the Czech Republic." Photograph. September 20, 2016. Accessed April 2023. Data sources for the creation of the map: Köppen types calculated from data from WorldClim.org. Wikimedia Commons. [https://cs.wikipedia.org/wiki/Soubor:CzechRepublic\\_koppen.svg](https://cs.wikipedia.org/wiki/Soubor:CzechRepublic_koppen.svg)
- [14] "The Köppen Climate Classification." Mindat.org. Accessed April 2023. <https://www.mindat.org/climate.php>
- [15] City of Broumov <https://goo.gl/maps/ygcCK8ygdySLkZ9y6>
- [16] Lukáš, Michl. 04/03/1979-11/30/2015 (unverified). Národní památkový ústav. Accessed April 2023. [https://iispp.npu.cz/mis\\_public/documentDetail.htm?id=1017533](https://iispp.npu.cz/mis_public/documentDetail.htm?id=1017533).
- [17] Slavík, Jiří. "Excursion 1: To the Building Development of the Current Deanery in Broumov." Průzkumy památek 22, no. 2/2015 (2015): 19–21. Accessed April 2023. <https://www.npu.cz/cs/e-shop/9394-pruzkumy-pamatek-ii-2015>
- [18] Dienstbier, Jan, Ondřej Faktor, and Jan Royt. "Medieval Wall Paintings in the Basement of the Broumov Parish." Průzkumy památek 22, no. 2/2015 (2015): 3–18. Accessed April 2023. <https://www.npu.cz/cs/e-shop/9394-pruzkumy-pamatek-ii-2015>
- [19] "BROUMOVSKÝ BIM INFORMAČNÍ MĚSÍČNÍK." Volume 14, issue 09, September 2022. Compiled by P. Martin Lanži, dean of ŘKF Broumov. Accessed April 2023. <https://www.broumovfarnost.cz/cs/bim-mesicnik/2022>
- [20] Tůmová, Štěpánka. "Farář hledal garáž, našel gotickou fresku. V Broumově ji ukazují po obnově." iDNES.cz/ZPRAVODAJSTVÍ. February 4, 2023. Accessed April 2023. [https://www.idnes.cz/hradec-kralove/zpravy/goticka-freska-posledni-soud-triumf-smrti-broumov-fara.A230131\\_701494\\_hradec-zpravy\\_tuu](https://www.idnes.cz/hradec-kralove/zpravy/goticka-freska-posledni-soud-triumf-smrti-broumov-fara.A230131_701494_hradec-zpravy_tuu).
- [21] Pykalová, Zuzana. 2001. Národní památkový ústav. October. Accessed April 2023. [https://iispp.npu.cz/mis\\_public/documentDetail.htm?id=42060](https://iispp.npu.cz/mis_public/documentDetail.htm?id=42060).



- [22] Levine, J.S., United States. National Park Service. Cultural Resources, and United States. National Park Service. Preservation Assistance Division. *The Repair, Replacement, and Maintenance of Historic Slate Roofs*. Preservation briefs. U.S. Department of the Interior, National Park Service, Cultural Resources, Preservation Assistance, 1993. Accessed June 2023. Available at: [https://books.google.cz/books?id=UqJt0bTZnTgC&printsec=frontcover&source=gbs\\_ge\\_s ummary\\_r&cad=0#v=onepage&q&f=false](https://books.google.cz/books?id=UqJt0bTZnTgC&printsec=frontcover&source=gbs_ge_s ummary_r&cad=0#v=onepage&q&f=false)
- [23] ICOMOS - ISCS. Illustrated Glossary on Stone Deterioration Patterns. English-Portuguese Version of 2008.
- [24] Barontini, Alberto, Maria Giovanna Masciotta, Luís F. Ramos, and Paulo B. Lourenço. "STRUCTURAL IDENTIFICATION AND MATERIAL CHARACTERISATION." Presentation slides, SA4: Inspection and Diagnosis, Advanced Masters in Structural Analysis of Monuments and Historical Constructions, UMinho University, Guimaraes, Portugal, November 2022.
- [25] Červenka, Vladimír, Libor Jendele, and Jan Červenka. ATENA Program Documentation Part 1: Theory. Prague: Červenka Consulting s.r.o., March 31, 2021.
- [26] Borri, Antonio, Marco Corradi, and Alessandro De Maria. "The Failure of Masonry Walls by Disaggregation and the Masonry Quality Index." *Heritage* 3, no. 4 (2020): 1162-1198. Accessed May, 2023. <https://doi.org/10.3390/heritage3040065>
- [27] Lourenço, Paulo B., and Angelo Gaetani. Finite Element Analysis for Building Assessment. First published in 2022. Routledge.
- [28] Waterproofing asphalt strip ELASTEK 40 SPECIAL MINERAL. DEK [Dekorativní chemie s.r.o.]. Accessed June 2023 <https://www.dek.cz/produkty/detail/1010151880-glastek-40-special-mineral-role-7-5m2/4663>
- [29] CEN. EN 1991-1-1: Eurocode 1: Actions on structures - Part 1-1: General actions - Densities, self-weight, imposed loads for buildings. 2022.
- [30] CEN. EN 1990:2002+A1:2005 Eurocode - Basis of Structural Design. 2005.
- [31] DLUBAL Software. "Snow Load Map of Czech Republic." Accessed April 2023. Available at: <https://www.dlubal.com/en/load-zones-for-snow-wind-earthquake/snow-csn-en-1991-1-3.html#&center=49.82002917199996,15.474952793374094&zoom=7&marker=50.075865,14.434609>.
- [32] Švorc, Jiří, Ing. Static Survey of the Broumov Parish House. January 2023.
- [33] Netinger Grubeša, Ivanka, Mihaela Teni, Hrvoje Krstić, and Martina Vračević. "Influence of Freeze/Thaw Cycles on Mechanical and Thermal Properties of Masonry Wall and Masonry Wall Materials." *Energies* 12, no. 8 (2019): 1464. <https://www.mdpi.com/1996-1073/12/8/1464>.
- [34] Nuno Mendes, Luís F. Ramos, and Paulo B. Lourenço " Non-destructive and minor destructive testing applied to masonry buildings." Presentation slides, SA4: Inspection and Diagnosis, Advanced Masters in Structural Analysis of Monuments and Historical Constructions, UMinho University, Guimaraes, Portugal, November 2022
- [35] Tiago Miranda, Luís F. Ramos, and Mandar Dewoolkar " IN SITU INVESTIGATION OF SOIL AND ROCKS." Presentation slides, SA4: Inspection and Diagnosis, Advanced Masters in Structural Analysis of Monuments and Historical Constructions, UMinho University, Guimaraes, Portugal, November 2022
- [36] CEN EN 1991-1-3:2003: Eurocode 1 - Actions on structures - Part 1-3: General actions - Snow loads. 2003

## **11. ANNEX**

### **11.1 Exterior Damage Mapping**



UNIVERSITY OF MINHO, PORTUGAL  
 CZECH TECHNICAL UNIVERSITY IN PRAGUE, CZECH REPUBLIC  
 UNIVERSITY OF PADOVA, ITALY  
 UNIVERSITY OF CATALONIA, SPAIN  
 INSTITUTE OF THEORETICAL AND APPLIED MECHANICS, CZECH REPUBLIC



Note:

Legend:

	Bristering
	Crack
	Craquele
	Delamination
	Discoloration
	Vegetation

Project title:  
 Evaluation of the Broumov parish house failure, its causality, and some ideas of remediation

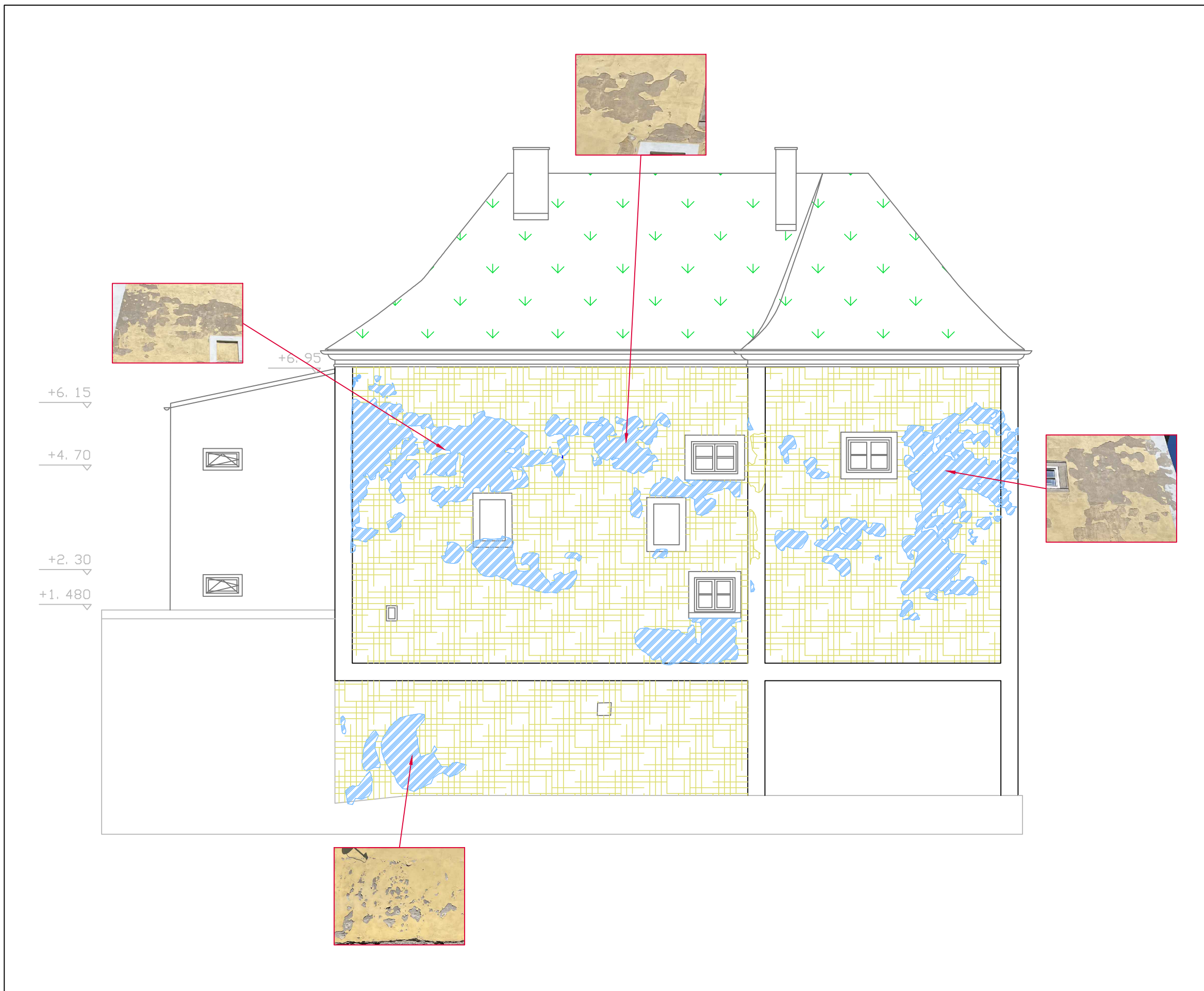
Drawing title:  
 Photographic Decay Survey of the Exterior  
 Northeast Façade

Scale: 1:1

Project carried out by:  
 ATHINA PAPADIAMANTI.

Supervisors:  
 Pavel Kuklik, Martin Valek, Petr Kabele

Drawing number: 01 | Sheet number: 1





UNIVERSITY OF MINHO, PORTUGAL  
 CZECH TECHNICAL UNIVERSITY IN PRAGUE, CZECH REPUBLIC  
 UNIVERSITY OF PADOVA, ITALY  
 UNIVERSITY OF CATALONIA, SPAIN  
 INSTITUTE OF THEORETICAL AND APPLIED MECHANICS, CZECH REPUBLIC



Note:

Legend:

	Bristering
	Crack
	Craquele
	Delamination
	Discoloration
	Vegetation

Project title:

Evaluation of the Broumov parish house failure, its causality, and some ideas of remediation

Drawing title:

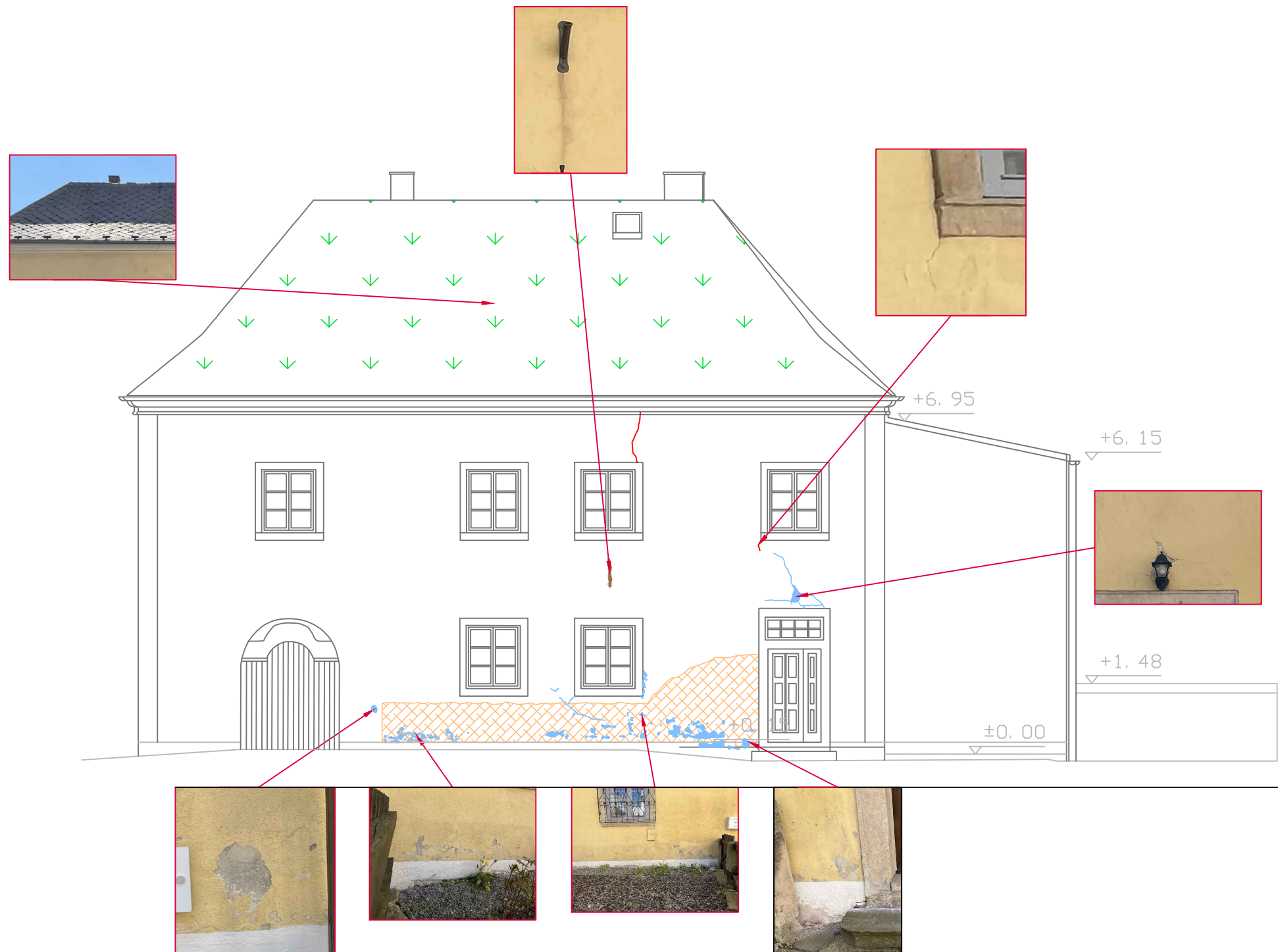
Photographic Decay Survey of the Exterior  
 Southwest Façade

Scale: 1:1

Project carried out by:  
 ATHINA PAPADIAMANTI.

Supervisors:  
 Pavel Kuklik, Martin Valek, Petr Kabele

Drawing number: 01 | Sheet number: 2





UNIVERSITY OF MINHO, PORTUGAL  
 CZECH TECHNICAL UNIVERSITY IN PRAGUE, CZECH REPUBLIC  
 UNIVERSITY OF PADOVA, ITALY  
 UNIVERSITY OF CATALONIA, SPAIN  
 INSTITUTE OF THEORETICAL AND APPLIED MECHANICS, CZECH REPUBLIC



Note:

Legend:

	<b>Bristering</b>
	<b>Crack</b>
	<b>Craquele</b>
	<b>Delamination</b>
	<b>Discoloration</b>
	<b>Vegetation</b>

Project title:

Evaluation of the Broumov parish house failure, its causality, and some ideas of remediation

Drawing title:

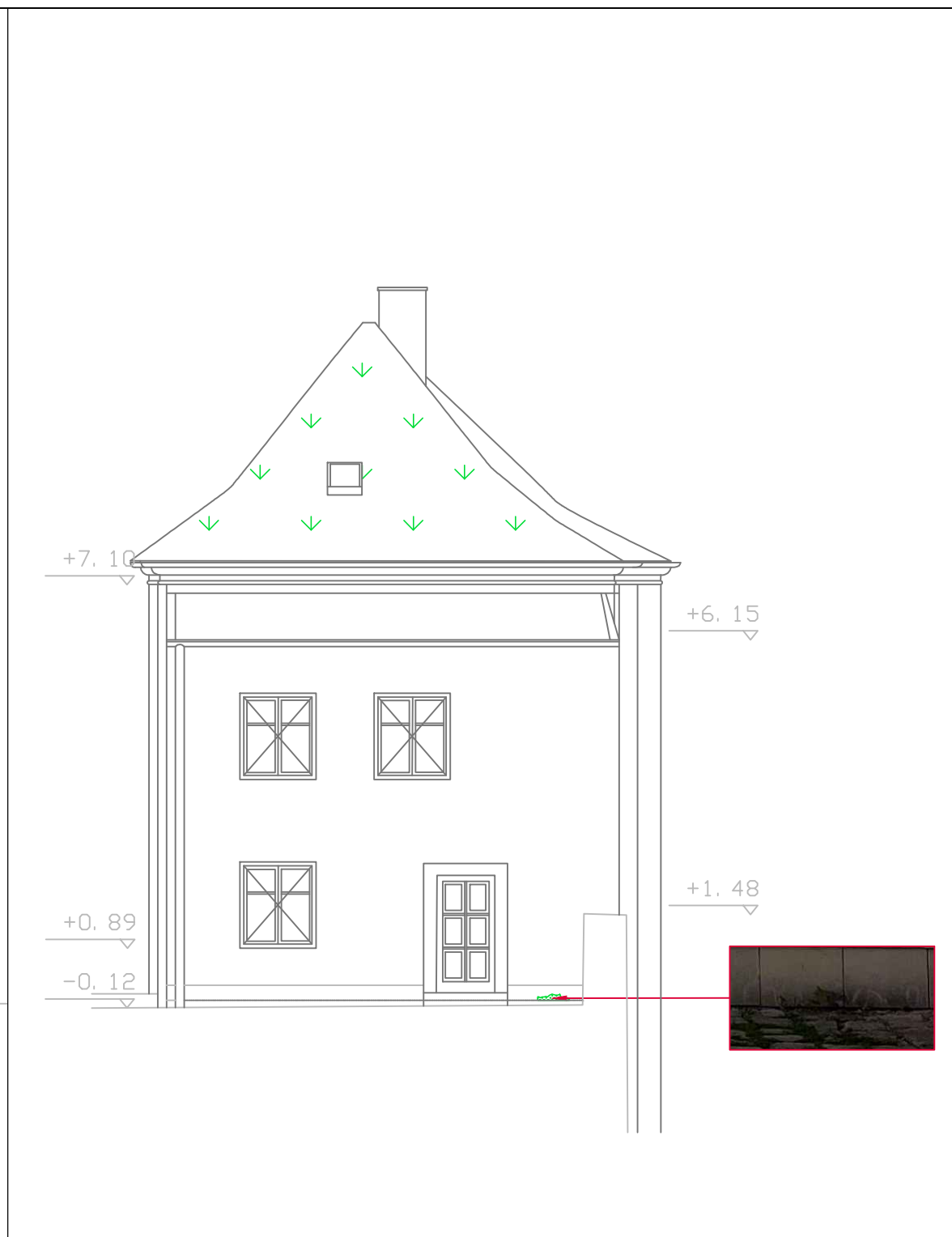
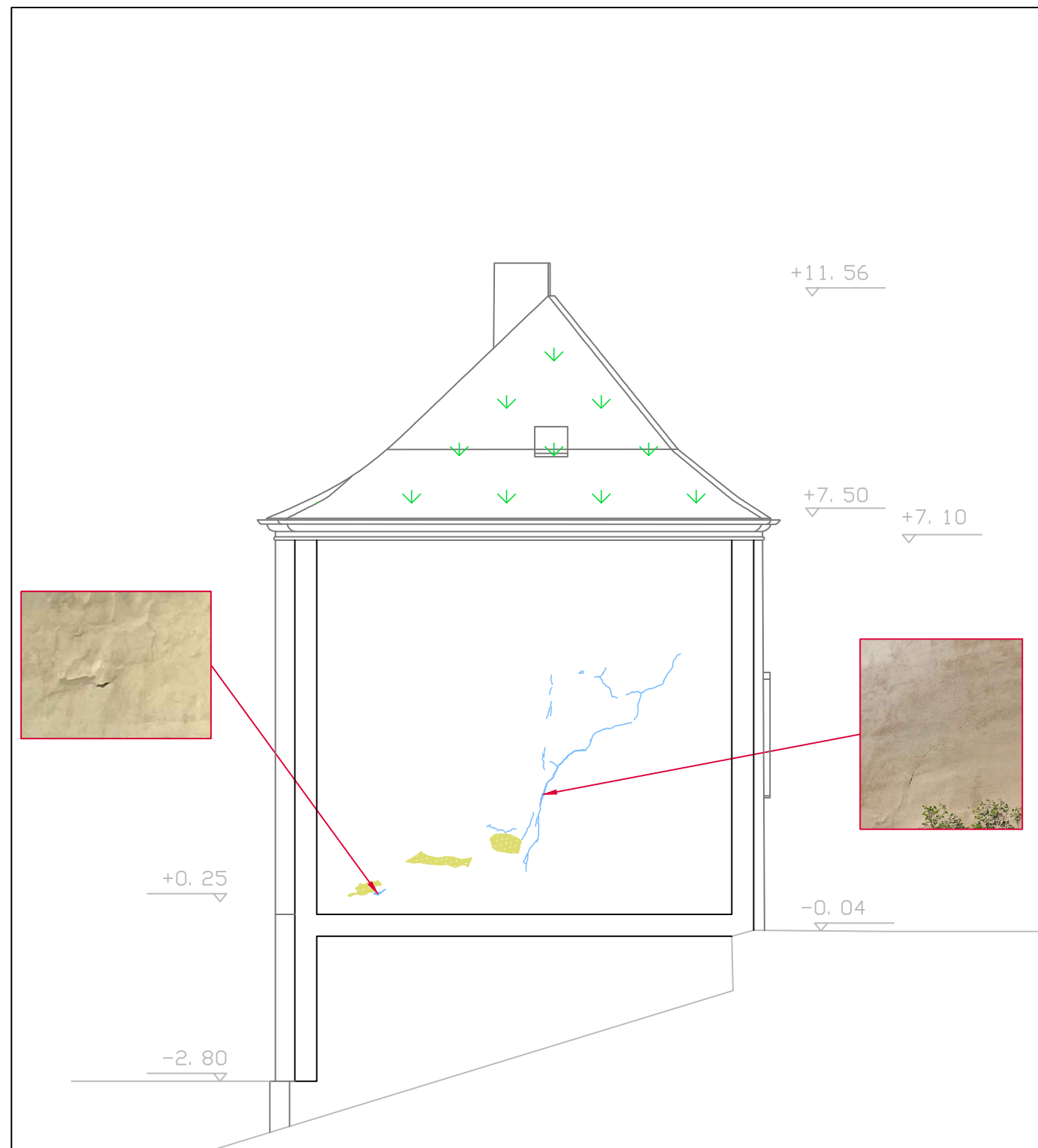
Photographic Decay Survey of the Exterior  
 Northwest & Southeast Façades

Scale: 1:1

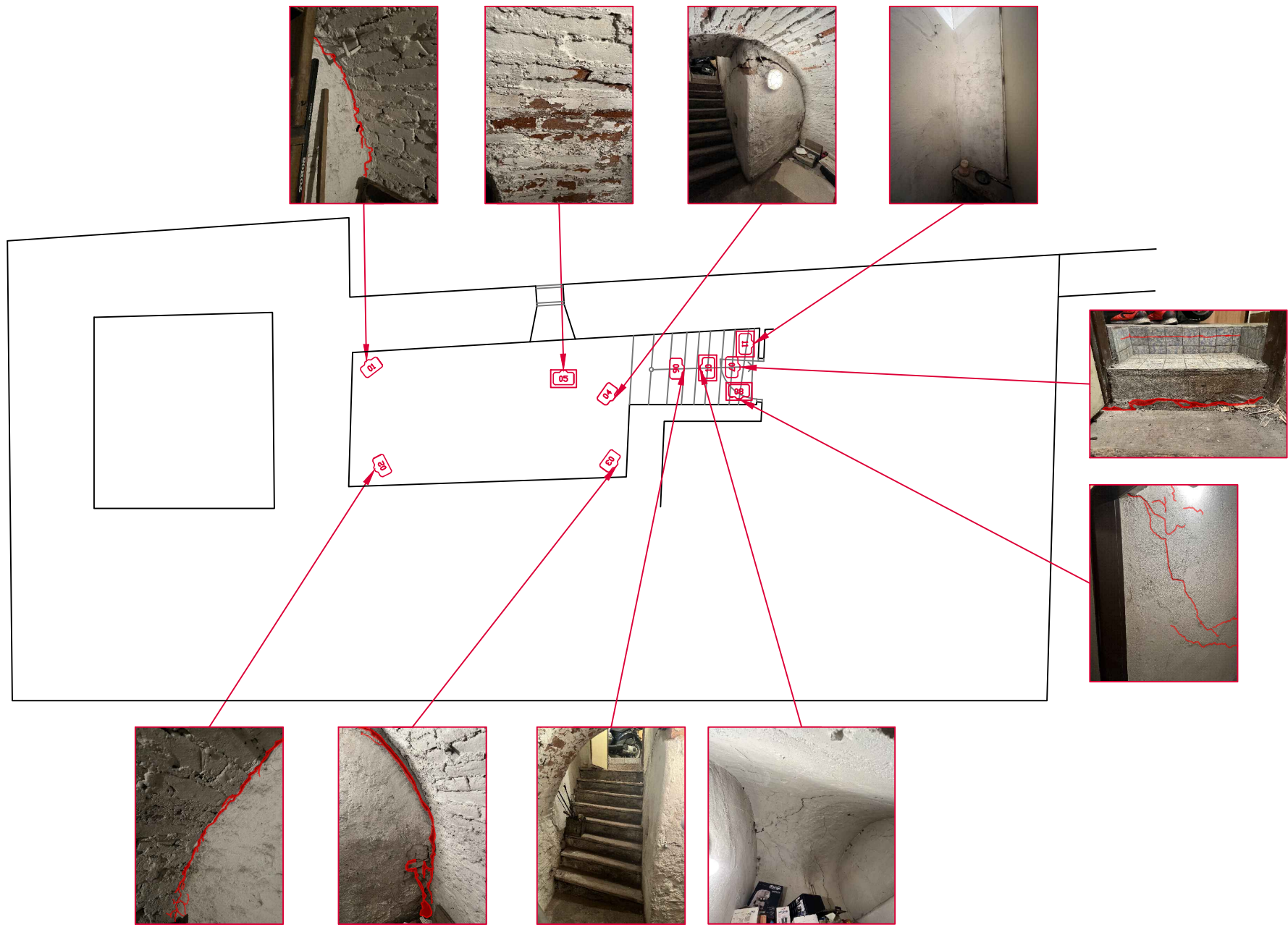
Project carried out by:  
 ATHINA PAPADIAMANTI.

Supervisors:  
 Pavel Kuklik, Martin Valek, Petr Kabele

Drawing number: 01 | Sheet number: 3



## **11.2 Interior Damage Mapping**

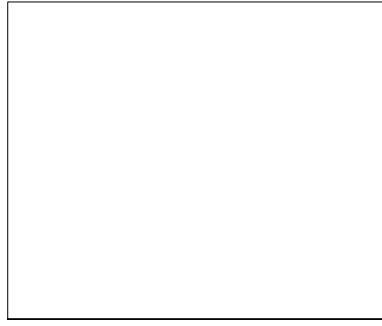


..NAYOUTUMINHO.jpg		
UNIVERSITY OF MINHO, PORTUGAL CZECH TECHNICAL UNIVERSITY IN PRAGUE, CZECH REPUBLIC UNIVERSITY OF PADOVA, ITALY UNIVERSITY OF CATALONIA, SPAIN INSTITUTE OF THEORETICAL AND APPLIED MECHANICS, CZECH REPUBLIC		



Note:

Legend:



Project title:  
Evaluation of the Broumov parish house failure, its causality, and some ideas of remediation

Drawing title:  
Photographic Decay Survey of the Interior Basement

Scale: 1:1

Project carried out by:  
ATHINA PAPADIAMANTI.

Supervisors:  
Pavel Kuklik, Martin Valek, Petr Kabele

Drawing number: 02 | Sheet number: 1



.Net\OUT\UNIND0.jpg			
UNIVERSITY OF MINHO, PORTUGAL CZECH TECHNICAL UNIVERSITY IN PRAGUE, CZECH REPUBLIC UNIVERSITY OF PADOVA, ITALY UNIVERSITY OF CATALONIA, SPAIN INSTITUTE OF THEORETICAL AND APPLIED MECHANICS, CZECH REPUBLIC			



Note:

---

Legend:

Project title:  
Evaluation of the Broumov parish house failure, its causality, and some ideas of remediation

Drawing title:  
Photographic Decay Survey of the Interior Ground Floor

Scale: 1:1

Project carried out by:  
ATHINA PAPADAMANTI.

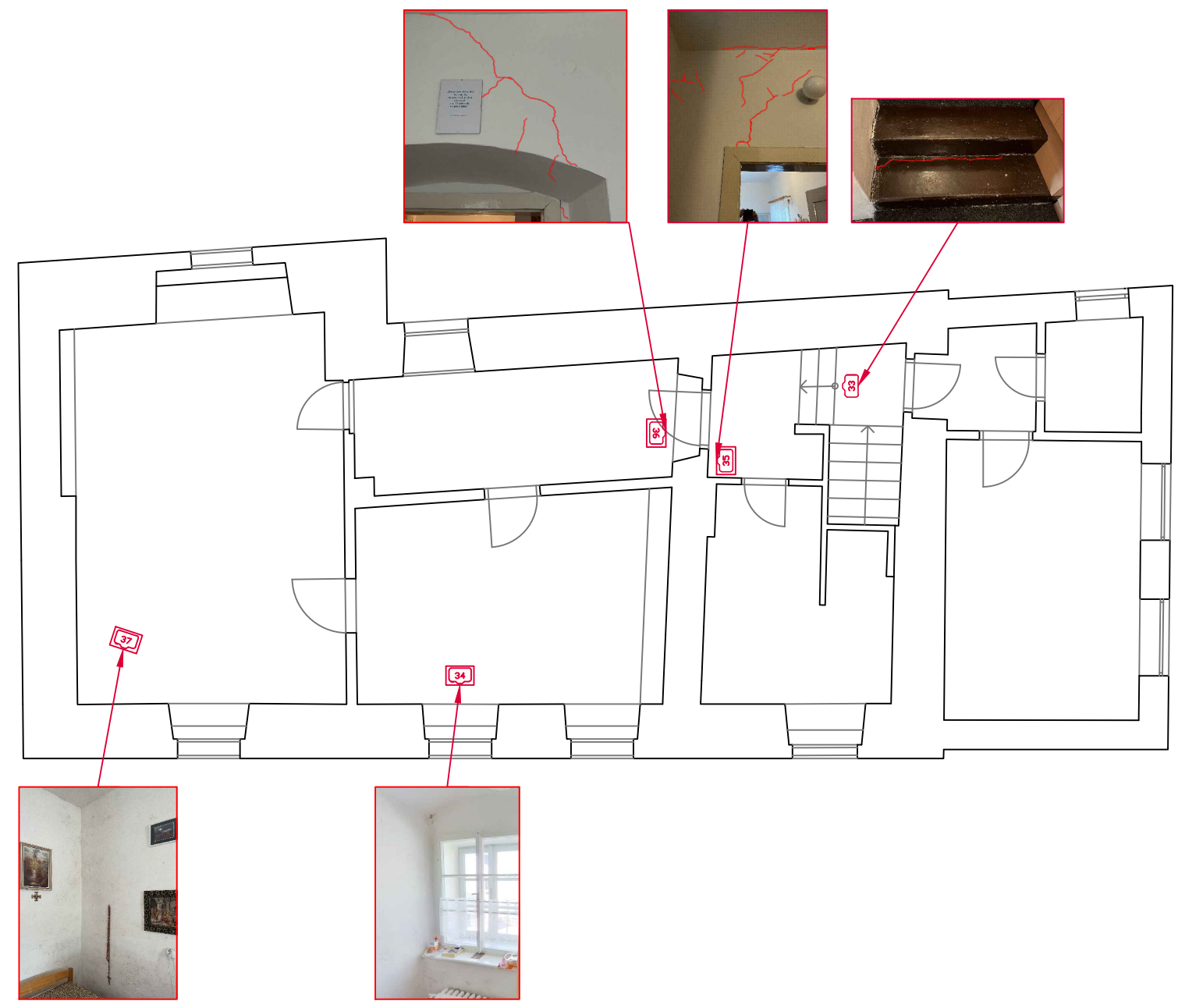
Supervisors:  
Pavel Kuklik, Martin Valek, Petr Kabele

Drawing number: 02 | Sheet number: 2





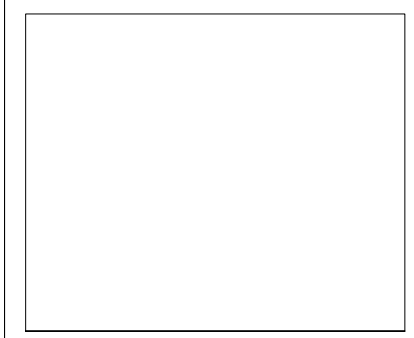
.Net\OUT\UNIDW0.jpg			
UNIVERSITY OF MINHO, PORTUGAL CZECH TECHNICAL UNIVERSITY IN PRAGUE, CZECH REPUBLIC UNIVERSITY OF PADOVA, ITALY UNIVERSITY OF CATALONIA, SPAIN INSTITUTE OF THEORETICAL AND APPLIED MECHANICS, CZECH REPUBLIC			



Note:

---

Legend:



Project title:  
Evaluation of the Broumov parish house failure, its causality, and some ideas of remediation

Drawing title:  
Photographic Decay Survey of the Interior  
1st Floor

Scale: 1:1

Project carried out by:  
ATHINA PAPADAMANTI.

Supervisors:  
Pavel Kuklik, Martin Valek, Petr Kabele

Drawing number: 02 | Sheet number: 3




### 11.3 Calculation of the roof's self-weight




Cross section		Area(m <sup>2</sup> )	Volume(m <sup>3</sup> )	Density (kg/m <sup>3</sup> )	Mass(kg)	g(N/kg)	Load(kN)
Length(m)	Width(m)						
0.18	0.2	2.33	4.66E-01	370	172.48	9.81	1.69E+00
0.16	0.2	0.13	6.40E-01	370	236.8	9.81	2.32E+00
0.13	0.15	1.32	1.99E-01	370	73.45	9.81	7.21E-01
0.12	0.14	0.91	1.09E-01	370	40.45	9.81	3.97E-01
0.11	0.14	0.39	5.52E-02	370	20.44	9.81	2.01E-01
SUM LOAD OF TRUSS							5.33E+00
SUM LOAD OF 5 TRUSSES							2.66E+01

Tiles	Area(m <sup>2</sup> )	Volume(m <sup>3</sup> )	Density (kg/m <sup>3</sup> )	Weight (kg/m <sup>2</sup> )	Mass(kg)	g(N/kg)	Load(kN)
Diamond shaped pattern of slates	0.25	1.15E-03	2600.00	-	2.99	9.81	2.93E-02
Waterproof asphalt strip GLASTEK 40 SPECIAL	0.25	-	-	4.50	1.04	9.81	1.02E-02
Roof batten with thickness 2 cm	0.25	4.70E-02	370.00		17.38	9.81	1.70E-01
SUM LOAD OF THE COVER							2.10E-01

SUM OF TRUSSES AND COVER	2.69E+01
<b>LOAD PER WALL</b>	<b>1.34E+01</b>

### 11.4 Calculation of the vaults' attached to the wall load

Photo	Location	Vault			Floor supported by the vault	Material Density (kg/m <sup>3</sup> )	Total Mass (kg)	g (N/kg)	Load (kN)	Distributed load (kN/m)
		Area (m <sup>2</sup> )	Thickness (m)	Volume (m <sup>3</sup> )	Volume (m <sup>3</sup> )					
	Administration room	0.86	0.9	0.774	3.0569	2000	7661.8	9.81	75.16	8.35E+01
	Hall	0.33	0.25	0.0825	0.096	2000	357	9.81	3.50	1.40E+01
	Hall	0.39	0.3	0.117	0.129	2000	492	9.81	4.83	1.61E+01

	Boiler room	0.37	0.5	0.185	0.1924	2000	754.8	9.81	7.41	1.48E+01
	Boiler room	0.71	0.2	0.141	0.0936	2000	469.2	9.81	4.60	2.30E+01
	Staircase to basement	0.15	0.9	0.135	0.5772	2000	1424.4	9.81	13.98	1.55E+01

## 11.5 Calculation of the snow 's live load

From the **EN 1991-1-3:2003** [36], the value of snow load is equal to:

$$s = \mu_1 * C_e * C_t * s_k$$

Where:

$\mu_1$  is the snow load shape coefficient

$s_k$  is the characteristic value of snow load on the ground

$C_e$  is the exposure coefficient

$C_t$  is the thermal coefficient

According to instructions of the **EN 1991-1-3:2003**  $C_e$  and  $C_t$  can be considered equal to 1 (Figure 11.1).

Table 5.1 Recommended values of $C_e$ for different topographies	
Topography	$C_e$
Windswept <sup>a</sup>	0,8
Normal <sup>b</sup>	1,0
Sheltered <sup>c</sup>	1,2

<sup>a</sup> *Windswept topography*: flat unobstructed areas exposed on all sides without, or little shelter afforded by terrain, higher construction works or trees.

<sup>b</sup> *Normal topography*: areas where there is no significant removal of snow by wind on construction work, because of terrain, other construction works or trees.

<sup>c</sup> *Sheltered topography*: areas in which the construction work being considered is considerably lower than the surrounding terrain or surrounded by high trees and/or surrounded by higher construction works.

(8) The thermal coefficient  $C_t$  should be used to account for the reduction of snow loads on roofs with high thermal transmittance ( $> 1 \text{ W/m}^2\text{K}$ ), in particular for some glass covered roofs, because of melting caused by heat loss.

For all other cases:

$C_t = 1,0$

**NOTE 1:** Based on the thermal insulating properties of the material and the shape of the construction work, the use of a reduced  $C_t$  value may be permitted through the National Annex.

**NOTE 2:** Further guidance may be obtained from ISO 4355.

Figure 11.1 - Recommended values of  $C_e$  and  $C_t$

The characteristic value of snow load  $s_k$  for the Broumov Region according to the Czech National Annexes is equal to  $2 \text{ kN/m}^2$ .

For the value of snow load shape coefficient  $\mu_1$ , Table 5.2 of the **EN 1991-1-3:2003** is used (Figure 11.2).

Table 5.2: Snow load shape coefficients			
Angle of pitch of roof $\alpha$	$0^\circ \leq \alpha \leq 30^\circ$	$30^\circ < \alpha < 60^\circ$	$\alpha \geq 60^\circ$
$\mu_1$	0,8	$0,8(60 - \alpha)/30$	0,0

Figure 11.2 - Table 5.2 of the EN1

$$\mu_1 = \frac{0,8 * (60 - 44)}{30} = 0.427$$

The total value of the snow live load is equal to:

$$s = 0,85 \text{ kN/m}^2$$

The value of the load that is transferred on each wall should be calculated. The total area that is taken into consideration is 38.76 m<sup>2</sup>. So the load acting for that area is 33.08 kN. This load is divided by two to find the value transferred to each wall is 16.54 KN.